

Scalable Robust Matrix Recovery: Frank-Wolfe Meets Proximal Methods

Cun Mu¹, Yuqian Zhang², John Wright², Donald Goldfarb¹

¹Department of Industrial Engineering and Operations Research, Columbia University

²Department of Electrical Engineering, Columbia University

November 26, 2021

Abstract

Recovering matrices from compressive and grossly corrupted observations is a fundamental problem in robust statistics, with rich applications in computer vision and machine learning. In theory, under certain conditions, this problem can be solved in polynomial time via a natural convex relaxation, known as Compressive Principal Component Pursuit (CPCP). However, all existing provable algorithms for CPCP suffer from superlinear per-iteration cost, which severely limits their applicability to large scale problems. In this paper, we propose provable, scalable and efficient methods to solve CPCP with (essentially) linear per-iteration cost. Our method combines classical ideas from Frank-Wolfe and proximal methods. In each iteration, we mainly exploit Frank-Wolfe to update the low-rank component with rank-one SVD and exploit the proximal step for the sparse term. Convergence results and implementation details are also discussed. We demonstrate the scalability of the proposed approach with promising numerical experiments on visual data.

1 Introduction

Suppose that a matrix $\mathbf{M}_0 \in \mathbb{R}^{m \times n}$ is generated as $\mathbf{M}_0 = \mathbf{L}_0 + \mathbf{S}_0 + \mathbf{N}_0$, where \mathbf{L}_0 is a low-rank matrix, \mathbf{S}_0 is a sparse error matrix, and \mathbf{N}_0 is a dense noise matrix. Linear measurements

$$\mathbf{b} = \mathcal{A}[\mathbf{M}_0] = (\langle \mathbf{A}_1, \mathbf{M}_0 \rangle, \langle \mathbf{A}_2, \mathbf{M}_0 \rangle, \dots, \langle \mathbf{A}_p, \mathbf{M}_0 \rangle)^* \in \mathbb{R}^p \quad (1.1)$$

are collected, where $\mathcal{A} : \mathbb{R}^{m \times n} \rightarrow \mathbb{R}^p$ is the sensing operator, \mathbf{A}_k is the sensing matrix for the k -th measurement and $\langle \mathbf{A}_k, \mathbf{M}_0 \rangle \doteq \text{Tr}(\mathbf{M}_0^* \mathbf{A}_k)$. *Can we, in a tractable way, recover \mathbf{L}_0 and \mathbf{S}_0 from \mathbf{b} with \mathcal{A} given?*

One natural approach is to solve the optimization

$$\min_{\mathbf{L}, \mathbf{S}} \frac{1}{2} \|\mathbf{b} - \mathcal{A}[\mathbf{L} + \mathbf{S}]\|_2^2 + \lambda_L \text{rank}(\mathbf{L}) + \lambda_S \|\mathbf{S}\|_0. \quad (1.2)$$

Here, λ_L and λ_S are regularization parameters, and $\|\mathbf{S}\|_0$ denotes the number of nonzero entries in \mathbf{S} .

Unfortunately, problem (1.2) is nonconvex, and hence is not directly tractable. However, by replacing the ℓ^0 norm $\|\mathbf{S}\|_0$ with the ℓ^1 norm $\|\mathbf{S}\|_1 \doteq \sum_{i=1}^m \sum_{j=1}^n |S_{ij}|$, and replacing the rank

$\text{rank}(\mathbf{L})$ with the nuclear norm $\|\mathbf{L}\|_*$ (i.e., the sum of the singular values of \mathbf{L}), we obtain a natural, tractable, convex relaxation of (1.2),

$$\min_{\mathbf{L}, \mathbf{S}} \frac{1}{2} \|\mathbf{b} - \mathcal{A}[\mathbf{L} + \mathbf{S}]\|_2^2 + \lambda_L \|\mathbf{L}\|_* + \lambda_S \|\mathbf{S}\|_1. \quad (1.3)$$

This optimization is sometimes referred to as *compressive principal component pursuit (CPCP)* [WGMM13]. Equivalently, since

$$\{ \mathbf{M} \in \mathbb{R}^{m \times n} \mid \mathbf{b} = \mathcal{A}[\mathbf{M}] \} = \{ \mathbf{M} \in \mathbb{R}^{m \times n} \mid \mathcal{P}_Q[\mathbf{M}] = \mathcal{P}_Q[\mathbf{M}_0] \},$$

where $\mathcal{Q} \subseteq \mathbb{R}^{m \times n}$ is a linear subspace spanned by $\{\mathbf{A}_i\}_{i=1}^p$, and \mathcal{P}_Q denotes the projection operator onto that subspace, we can rewrite problem (1.3) in a (possibly) more compact form¹

$$\min_{\mathbf{L}, \mathbf{S}} f(\mathbf{L}, \mathbf{S}) \doteq \frac{1}{2} \|\mathcal{P}_Q[\mathbf{L} + \mathbf{S} - \mathbf{M}_0]\|_F^2 + \lambda_L \|\mathbf{L}\|_* + \lambda_S \|\mathbf{S}\|_1. \quad (1.4)$$

Recently, CPCP and its near variants have been studied for different sensing operators \mathcal{A} (or equivalently different subspaces \mathcal{Q}). In specific, [CSPW11, CLMW11, ZLW⁺10, HKZ11, ANW12] considers the case where a subset $\Omega \subseteq \{1, 2, \dots, m\} \times \{1, 2, \dots, n\}$ of the entries of \mathbf{M}_0 is observed. Then CPCP can be reduced to

$$\min_{\mathbf{L}, \mathbf{S}} \frac{1}{2} \|\mathcal{P}_\Omega[\mathbf{L} + \mathbf{S} - \mathbf{M}_0]\|_F^2 + \lambda_L \|\mathbf{L}\|_* + \lambda_S \|\mathbf{S}\|_1, \quad (1.5)$$

where $\mathcal{P}_\Omega[\cdot]$ denotes the orthogonal projection onto the linear space of matrices supported on Ω , i.e., $\mathcal{P}_\Omega[\mathbf{M}_0](i, j) = (\mathbf{M}_0)_{ij}$ if $(i, j) \in \Omega$ and $\mathcal{P}_\Omega[\mathbf{M}_0](i, j) = 0$ otherwise. [WGMM13] studies the case where each \mathcal{A}_k is a iid $\mathcal{N}(0, 1)$ matrix, which is equivalent (in distribution) to saying that we choose a linear subspace \mathcal{Q} uniformly at random from the set of all p -dimensional subspaces of $\mathbb{R}^{m \times n}$ and observe $\mathcal{P}_Q[\mathbf{M}_0]$. Consentaneously, all the above works manage to provide theoretical guarantees for CPCP, under fairly mild conditions, to produce accurate estimates of \mathbf{L}_0 and $\mathcal{P}_\Omega[\mathbf{S}_0] / \mathbf{S}_0$, even when the number of measurements p is much less than mn .

Inspired by these theoretical results, researchers from different fields have leveraged CPCP to solve many practical problems, including video background modeling [CLMW11], batch image alignment [PGW⁺12], face verification [ZMKW13], photometric stereo [WGS⁺11], dynamic MRI [OCS13], topic modeling [MZWM10], latent variable graphical model learning [CPW12] and outlier detection and robust Principal Component Analysis [CLMW11], just to name a few.

Living in the era of “big data”, most of these applications involve large datasets and high dimensional data spaces. Therefore, to fully realize the benefit of the theory, we need *provable* and *scalable* algorithms for CPCP. This has motivated a large number of works on developing first-order methods for problem (1.4) and its variants, e.g. [LGW⁺09, LCM10, YY09, AGI11, TY11, AGM12]. These methods all exploit a closed-form expression for the proximal operator of nuclear norm, which involves the singular value decomposition (SVD). Hence, the dominant cost in each iteration is computing an SVD of the same size as the input data. This is substantially more scalable than

¹ To transform problem (1.3) into problem (1.4), simple procedures like Gram-chmidt might be invoked. Despite being equivalent, one formulation might be preferred over the other in practice, depending on the specifications of sensing operator $\mathcal{A}[\cdot]$. In this paper, we will mainly focus on solving problem (1.4) and its variant. Our methods, however, are not restrictive to (1.4) at all and can be easily extended to problem (1.3).

off-the-shelf interior point solvers such as SDPT3 [TTT03]. Nevertheless, the superlinear cost of each iteration has limited their practical applicability to problems involving several thousands of data points and several thousands of dimensions. The need to compute a sequence of full or partial SVD's is a serious bottleneck for large scale applications.

As a remedy, in this paper, we design more scalable algorithms to solve CPCP with only a rank-one SVD in each iteration. Our approach leverages two classical and widely studied ideas – Frank-Wolfe iterations to handle the nuclear norm, and proximal steps to handle the ℓ_1 norm. This turns out to be precisely the right combination of techniques to solve CPCP at a very large scale. In particular, it yields algorithms that are substantially more scalable than prox-based first-order methods such as ISTA and FISTA [BT09], and converge much quicker in practice than a straightforward application of Frank-Wolfe.

The remainder of this paper is organized as follows. Section 2 reviews the general properties of the Frank-Wolfe algorithm, and describes several basic building blocks that we will use in our algorithms. Section 3 and Section 4 respectively describe how to modify the Frank-Wolfe algorithm to solve CPCP's norm constrained version

$$\min_{\mathbf{L}, \mathbf{S}} l(\mathbf{L}, \mathbf{S}) \doteq \frac{1}{2} \|\mathcal{P}_Q[\mathbf{L} + \mathbf{S} - \mathbf{M}_0]\|_F^2 \quad \text{s.t.} \quad \|\mathbf{L}\|_* \leq \tau_L, \|\mathbf{S}\|_1 \leq \tau_S, \quad (1.6)$$

and the penalized version, i.e. problem (1.4), by incorporating proximal regularization to more effectively handle the ℓ_1 norm. Convergence results and our implementation details are also discussed. Section 5 presents numerical experiments on large datasets that demonstrate the scalability of our proposed algorithms.

2 Preliminaries

2.1 Frank-Wolfe method

The Frank-Wolfe (FW) method [FW56], also known as the conditional gradient method [LP66], pertains to the general problem of minimizing a differentiable convex function h over a compact, convex domain $\mathcal{D} \subseteq \mathbb{R}^n$:

$$\text{minimize} \quad h(\mathbf{x}) \quad \text{subject to} \quad \mathbf{x} \in \mathcal{D} \subseteq \mathbb{R}^n. \quad (2.1)$$

Here, ∇h is assumed to be L -Lipschitz:

$$\forall \mathbf{x}, \mathbf{y} \in \mathcal{D}, \quad \|\nabla h(\mathbf{x}) - \nabla h(\mathbf{y})\| \leq L \|\mathbf{x} - \mathbf{y}\|. \quad (2.2)$$

Throughout, we let $D = \max_{\mathbf{x}, \mathbf{y} \in \mathcal{D}} \|\mathbf{x} - \mathbf{y}\|$ denote the diameter of the feasible set \mathcal{D} .

In its simplest form, the Frank-Wolfe algorithm proceeds as follows. At each iteration k , we linearize the objective function h about the current point \mathbf{x}^k :

$$h(\mathbf{v}) \approx h(\mathbf{x}^k) + \langle \nabla h(\mathbf{x}^k), \mathbf{v} - \mathbf{x}^k \rangle. \quad (2.3)$$

We minimize the linearization over the feasible set \mathcal{D} to obtain a feasible descent direction $\mathbf{v}^k - \mathbf{x}^k$ and then step in this direction:

$$\mathbf{x}^{k+1} = \mathbf{x}^k + \frac{2}{k+2} (\mathbf{v}^k - \mathbf{x}^k). \quad (2.4)$$

Algorithm 1 Frank-Wolfe method for problem (2.1)

```

1: Initialization:  $\mathbf{x}^0 \in \mathcal{D}$ ;
2: for  $k = 0, 1, 2, \dots$  do
3:    $\mathbf{v}^k \in \operatorname{argmin}_{\mathbf{v} \in \mathcal{D}} \langle \mathbf{v}, \nabla h(\mathbf{x}^k) \rangle$ ;
4:    $\gamma = \frac{2}{k+2}$ ;
5:    $\mathbf{x}^{k+1} = \mathbf{x}^k + \gamma(\mathbf{v}^k - \mathbf{x}^k)$ ;
6: end for

```

This yields a very simple procedure, which we summarize as Algorithm 1. The particular step size, $\frac{2}{k+2}$, comes from the convergence analysis of the algorithm, which we discuss in more detail below.

First proposed in [FW56], FW-type methods have been frequently revisited in different fields. Recently, they have experienced a resurgence in statistics, machine learning and signal processing, due to their ability to yield highly scalable algorithms for optimization with structure-encouraging norms such as the ℓ_1 norm and nuclear norm. In particular, if \mathbf{x} is a matrix and $\mathcal{D} = \{\mathbf{x} \mid \|\mathbf{x}\|_* \leq \beta\}$ is a nuclear norm ball, the subproblem

$$\min_{\mathbf{v} \in \mathcal{D}} \langle \mathbf{v}, \nabla h(\mathbf{x}) \rangle \quad (2.5)$$

can be solved using only the singular vector pair corresponding to the single leading singular value of the matrix $\nabla h(\mathbf{x})$. Thus, at each iteration, we only have to compute a rank-one partial SVD. This is substantially cheaper than the full/partial SVD exploited in proximal methods [JS10, HJN13]. We recommend [Jag13] as a comprehensive survey of the latest developments in FW-type methods.

In the past five decades, numerous variants of Algorithm 1 have been proposed and implemented. Many modify Algorithm 1 by replacing the simple updating rule (2.4) with more sophisticated schemes, e.g.,

$$\mathbf{x}^{k+1} \in \operatorname{argmin}_{\mathbf{x}} h(\mathbf{x}) \quad \text{s.t. } \mathbf{x} \in \operatorname{conv}\{\mathbf{x}^k, \mathbf{v}^k\} \quad (2.6)$$

or

$$\mathbf{x}^{k+1} \in \operatorname{argmin}_{\mathbf{x}} h(\mathbf{x}) \quad \text{s.t. } \mathbf{x} \in \operatorname{conv}\{\mathbf{x}^k, \mathbf{v}^k, \mathbf{v}^{k-1}, \dots, \mathbf{v}^{k-j}\}. \quad (2.7)$$

The convergence of these schemes can be analyzed simultaneously, using the fact that they produce iterates \mathbf{x}^{k+1} whose objective is no greater than that produced by the original Frank-Wolfe update scheme:

$$h(\mathbf{x}^{k+1}) \leq h(\mathbf{x}^k + \gamma(\mathbf{v}^k - \mathbf{x}^k)).$$

Algorithm 2 states a general version of Frank-Wolfe, whose update is only required to satisfy this relationship. It includes as special cases the updating rules (2.4), (2.6) and (2.7). This flexibility will be crucial for effectively handling the sparse structure in the CPCP problems (1.4) and (1.6).

Algorithm 2 Frank-Wolfe method for problem (2.1) with general updating scheme

```

1: Initialization:  $\mathbf{x}^0 \in \mathcal{D}$ ;
2: for  $k = 0, 1, 2, \dots$  do
3:    $\mathbf{v}^k \in \operatorname{argmin}_{\mathbf{v} \in \mathcal{D}} \langle \mathbf{v}, \nabla h(\mathbf{x}^k) \rangle$ ;
4:    $\gamma = \frac{2}{k+2}$ ;
5:   Update  $\mathbf{x}^{k+1}$  to some point in  $\mathcal{D}$  such that  $h(\mathbf{x}^{k+1}) \leq h(\mathbf{x}^k + \gamma(\mathbf{v}^k - \mathbf{x}^k))$ ;
6: end for

```

The convergence of Algorithm 2 can be proved using well-established techniques [HJN13, Jag13, DR70, DH78, Pat93, Zha03, Cla10]. Using these ideas, we can show that it converges at a rate of $O(1/k)$ in function value:

Theorem 1. *Let \mathbf{x}^* be an optimal solution to (2.1). For $\{\mathbf{x}^k\}$ generated by Algorithm 2, we have for $k = 0, 1, 2, \dots$,*

$$h(\mathbf{x}^k) - h(\mathbf{x}^*) \leq \frac{2LD^2}{k+2}. \quad (2.8)$$

Note that the constant on the rate of convergence depends on the Lipschitz constant L of h and the diameter \mathcal{D} . This result was perhaps first derived by [DR70]. For completeness, we provide a proof of Theorem 1 in the appendix.

While Theorem 1 guarantees that Algorithm 2 converges at a rate of $O(1/k)$, in practice it is useful to have a more precise bound on the suboptimality at iterate k . The surrogate duality gap

$$d(\mathbf{x}^k) = \langle \mathbf{x}^k - \mathbf{v}^k, \nabla h(\mathbf{x}^k) \rangle, \quad (2.9)$$

provides a useful upper bound on the suboptimality $h(\mathbf{x}^k) - h(\mathbf{x}^*)$:

$$\begin{aligned} h(\mathbf{x}^k) - h(\mathbf{x}^*) &\leq -\langle \mathbf{x}^* - \mathbf{x}^k, \nabla h(\mathbf{x}^k) \rangle \\ &\leq -\min_{\mathbf{v}} \langle \mathbf{v} - \mathbf{x}^k, \nabla h(\mathbf{x}^k) \rangle = \langle \mathbf{x}^k - \mathbf{v}^k, \nabla h(\mathbf{x}^k) \rangle = d(\mathbf{x}^k). \end{aligned} \quad (2.10)$$

The quantity $d(\mathbf{x}^k)$ was proposed in [Jag13]; see also [Cla10]. Theorem 2 of [Jag13] shows that $d(\mathbf{x}^k) = O(1/k)$. In the appendix, we prove the following refinement of this result, using ideas from [Jag13, Cla10]:

Theorem 2. *Let $\{\mathbf{x}^k\}$ be the sequence generated by Algorithm 2. Then for any $K \geq 1$, there exists $1 \leq \tilde{k} \leq K$ such that*

$$d(\mathbf{x}^{\tilde{k}}) \leq \frac{6LD^2}{K+2}. \quad (2.11)$$

Since this matches the worst case convergence rate for $h(\mathbf{x}^k) - h(\mathbf{x}^*)$, it suggests that the upper bound $d(\mathbf{x}^k)$ provides a valid stopping criterion in practice.

For our problem, the main computational burden in Algorithms 1 and 2 will be solving the linear subproblem $\min_{\mathbf{v} \in \mathcal{D}} \langle \mathbf{v}, \nabla h(\mathbf{x}^k) \rangle$.² To solve this problem, we will need to be able to efficiently minimize linear functions over the unit balls for $\|\cdot\|_*$ and $\|\cdot\|_1$. Fortunately, both of these operations have closed-form solutions, which we will describe in the next section.

2.2 Optimization oracles

In this part, we describe several optimization oracles involving ℓ_1 norm and nuclear norm, which serve as the main building blocks for our methods. These oracles are easy to compute and have computational cost (essentially) linear in the size of the input.

²In some situations, we can significantly reduce this cost by solving this problem inexactly [DH78, Jag13]. Our algorithms and results can also tolerate inexact step calculations; we omit the discussion here for simplicity.

Minimizing a linear function over the nuclear norm ball. Since the dual norm of the nuclear norm is the operator norm, i.e., $\|\mathbf{Y}\| = \max_{\|\mathbf{X}\|_* \leq 1} \langle \mathbf{Y}, \mathbf{X} \rangle$, the optimization problem

$$\text{minimize}_{\mathbf{X}} \langle \mathbf{Y}, \mathbf{X} \rangle \quad \text{subject to } \|\mathbf{X}\|_* \leq 1 \quad (2.12)$$

has optimal value $-\|\mathbf{Y}\|$. One minimizer is the rank-one matrix $\mathbf{X}^* = -\mathbf{u}\mathbf{v}^\top$, where \mathbf{u} and \mathbf{v} are the left- and right- singular vectors corresponding to the leading singular value of \mathbf{Y} .

Minimizing a linear function over the ℓ^1 ball. Since the dual norm of the ℓ_1 norm is the ℓ_∞ norm, i.e., $\|\mathbf{Y}\|_\infty := \max_{(i,j)} |Y_{ij}| = \max_{\|\mathbf{X}\|_1 \leq 1} \langle \mathbf{Y}, \mathbf{X} \rangle$, the optimization problem

$$\text{minimize}_{\mathbf{X}} \langle \mathbf{Y}, \mathbf{X} \rangle \quad \text{subject to } \|\mathbf{X}\|_1 \leq 1 \quad (2.13)$$

has optimal value $-\|\mathbf{Y}\|_\infty$. One minimizer is the one-sparse matrix $\mathbf{X}^* = -\mathbf{e}_i \mathbf{e}_j^*$, where $(i^*, j^*) \in \arg \max_{(i,j)} |Y_{ij}|$.

Projection onto the ℓ_1 -ball. To effectively handle the sparse term in the norm constrained problem (1.6), we will need to modify the Frank-Wolfe algorithm by incorporating additional projection steps. For any $\mathbf{Y} \in \mathbb{R}^{m \times n}$ and $\beta > 0$, the projection onto the ℓ_1 -ball:

$$\mathcal{P}_{\|\cdot\|_1 \leq \beta}[\mathbf{Y}] = \arg \min_{\|\mathbf{X}\|_1 \leq \beta} \frac{1}{2} \|\mathbf{X} - \mathbf{Y}\|_F^2, \quad (2.14)$$

can be easily solved with $O(mn(\log m + \log n))$ cost [DSSSC08]. Moreover, a divide and conquer algorithm, achieving linear cost in expectation to solve (2.14), has also been proposed in [DSSSC08].

Proximal mapping of ℓ_1 norm. To effectively handle the sparse term arising in problem (1.4), we will need to modify the Frank-Wolfe algorithm by incorporating additional proximal steps. For any $\mathbf{Y} \in \mathbb{R}^{m \times n}$ and $\lambda > 0$, the proximal mapping of ℓ_1 norm has the following closed-form expression

$$\mathcal{T}_\lambda[\mathbf{Y}] = \arg \min_{\mathbf{X} \in \mathbb{R}^{m \times n}} \frac{1}{2} \|\mathbf{X} - \mathbf{Y}\|_F^2 + \lambda \|\mathbf{X}\|_1, \quad (2.15)$$

where $\mathcal{T}_\lambda : \mathbb{R} \rightarrow \mathbb{R}$ denotes the soft-thresholding operator $\mathcal{T}_\lambda(x) = \text{sgn}(x) \max\{|x| - \lambda, 0\}$, and extension to matrices is obtained by applying the scalar operator $\mathcal{T}_\lambda(\cdot)$ to each element.

3 FW-P Method for Norm Constrained Problem

In this section, we develop scalable algorithms for the norm-constrained compressive principal component pursuit problem,

$$\min_{\mathbf{L}, \mathbf{S}} l(\mathbf{L}, \mathbf{S}) = \frac{1}{2} \|\mathcal{P}_Q[\mathbf{L} + \mathbf{S} - \mathbf{M}]\|_F^2 \quad \text{s.t.} \quad \|\mathbf{L}\|_* \leq \tau_L, \|\mathbf{S}\|_1 \leq \tau_S. \quad (3.1)$$

We first describe a straightforward application of the Frank-Wolfe method to this problem. We will see that although it has relatively cheap iterations, it converges very slowly on typical numerical examples, because it only makes a one-sparse update on the sparse term \mathbf{S} at a time. We will show how to remedy this problem by augmenting the FW iteration with an additional proximal step (essentially projected gradient here) in each iteration, yielding a new algorithm which updates \mathbf{S} much more efficiently. Because it combines Frank-Wolfe and projection steps, we will call this new algorithm Frank-Wolfe-Projection(FW-P).

Properties of the objective and constraints. To apply Frank-Wolfe to (3.1), we first note that the objective $l(\mathbf{L}, \mathbf{S})$ in (3.1) is differentiable, with

$$\nabla_{\mathbf{L}} l(\mathbf{L}, \mathbf{S}) = \mathcal{P}_Q[\mathbf{L} + \mathbf{S} - \mathbf{M}] \quad (3.2)$$

$$\nabla_{\mathbf{S}} l(\mathbf{L}, \mathbf{S}) = \mathcal{P}_Q[\mathbf{L} + \mathbf{S} - \mathbf{M}]. \quad (3.3)$$

A calculation, which we summarize as the following lemma, shows that the gradient map $\nabla l(\mathbf{L}, \mathbf{S}) = (\nabla_{\mathbf{L}} l, \nabla_{\mathbf{S}} l)$ is 2-Lipschitz:

Lemma 1. *For all (\mathbf{L}, \mathbf{S}) and $(\mathbf{L}', \mathbf{S}')$, $\|\nabla l(\mathbf{L}, \mathbf{S}) - \nabla l(\mathbf{L}', \mathbf{S}')\|_F \leq 2\|(\mathbf{L}, \mathbf{S}) - (\mathbf{L}', \mathbf{S}')\|_F$.*

The feasible set in (3.1) is compact. The following lemma bounds its diameter D :

Lemma 2. *The feasible set $\mathcal{D} = \{(\mathbf{L}, \mathbf{S}) \mid \|\mathbf{L}\|_* \leq \tau_L, \|\mathbf{S}\|_1 \leq \tau_S\}$ has diameter $D \leq 2\sqrt{\tau_L^2 + \tau_S^2}$.*

3.1 Frank-Wolfe for problem (3.1)

Since (3.1) asks us to minimize a convex, differentiable function with Lipschitz gradient over a compact convex domain, the Frank-Wolfe method in Algorithm 1 applies. It generates a sequence of iterates $\mathbf{x}^k = (\mathbf{L}^k, \mathbf{S}^k)$. Using the expression for the gradient in (3.2)-(3.3), at each iteration, the step direction $\mathbf{v}^k = (\mathbf{V}_L^k, \mathbf{V}_S^k)$ is generated by solving the linearized subproblem

$$\begin{aligned} \begin{pmatrix} \mathbf{V}_L^k \\ \mathbf{V}_S^k \end{pmatrix} \in \arg \min \quad & \left\langle \begin{pmatrix} \mathcal{P}_Q[\mathbf{L}^k + \mathbf{S}^k - \mathbf{M}] \\ \mathcal{P}_Q[\mathbf{L}^k + \mathbf{S}^k - \mathbf{M}] \end{pmatrix}, \begin{pmatrix} \mathbf{V}_L \\ \mathbf{V}_S \end{pmatrix} \right\rangle \\ \text{s.t.} \quad & \|\mathbf{V}_L\|_* \leq \tau_L, \|\mathbf{V}_S\|_1 \leq \tau_S. \end{aligned} \quad (3.4)$$

The problem (3.4) decouples into two independent subproblems:

$$\begin{aligned} \mathbf{V}_L^k &\in \arg \min_{\|\mathbf{V}_L\|_* \leq \tau_L} \langle \mathcal{P}_Q[\mathbf{L}^k + \mathbf{S}^k - \mathbf{M}], \mathbf{V}_L \rangle, \\ \mathbf{V}_S^k &\in \arg \min_{\|\mathbf{V}_S\|_1 \leq \tau_S} \langle \mathcal{P}_Q[\mathbf{L}^k + \mathbf{S}^k - \mathbf{M}], \mathbf{V}_S \rangle. \end{aligned}$$

These subproblems can be easily solved by exploiting the linear optimization oracles introduced in Section 2.2. In particular, we can take

$$\mathbf{V}_L^k = -\tau_L \mathbf{u}^k (\mathbf{v}^k)^*, \quad (3.5)$$

$$\mathbf{V}_S^k = -\tau_S \mathbf{e}_{i^*}^k (\mathbf{e}_{j^*}^k)^*, \quad (3.6)$$

where \mathbf{u}^k and \mathbf{v}^k are leading left- and right- singular vectors of $\mathcal{P}_Q[\mathbf{L}^k + \mathbf{S}^k - \mathbf{M}]$ and (i^*, j^*) index the largest element of $\mathcal{P}_Q[\mathbf{L}^k + \mathbf{S}^k - \mathbf{M}]$ in magnitude. Algorithm 3 summarizes the resulting algorithm.

The major advantage of Algorithm 3 derives from the simplicity of the update rules (3.5)-(3.6). Both have closed form, and both can be computed in time (essentially) linear in the size of the input. Because \mathbf{V}_L^k is rank-one, the algorithm can be viewed as performing a sequence of rank one updates.

The major disadvantage of Algorithm 3 is that \mathbf{S} has only a one-sparse update at a time, since $\mathbf{V}_S^k = -\tau_S \mathbf{e}_{i^*}^k (\mathbf{e}_{j^*}^k)^*$ has only one nonzero entry. This is a significant disadvantage in practice, as the optimal \mathbf{S}^* may have a relatively large number of nonzero entries. Indeed, in theory, the CPCP relaxation works even when a constant fraction of the entries in \mathbf{S}_0 are nonzero. In applications such as foreground-background separation, the number of nonzero entries in the target sparse term can be quite large. The red curves in Figure 2 show the effect of this on the practical convergence of the algorithm, on a simulated example of size $1,000 \times 1,000$, in which about 1% of the entries in the target sparse matrix \mathbf{S}_0 are nonzero. As shown, the progress is quite slow.

Algorithm 3 Frank-Wolfe method for problem (3.1)

```

1: Initialization:  $\mathbf{L}^0 = \mathbf{S}^0 = \mathbf{0}$ ;
2: for  $k = 0, 1, 2, \dots$  do
3:    $\mathbf{D}_L^k \in \arg \min_{\|\mathbf{D}_L\|_* \leq 1} \langle \mathcal{P}_Q[\mathbf{L}^k + \mathbf{S}^k - \mathbf{M}], \mathbf{D}_L \rangle$ ;  $\mathbf{V}_L^k = \tau_L \mathbf{D}_L^k$ ;
4:    $\mathbf{D}_S^k \in \arg \min_{\|\mathbf{D}_S\|_1 \leq 1} \langle \mathcal{P}_Q[\mathbf{L}^k + \mathbf{S}^k - \mathbf{M}], \mathbf{D}_S \rangle$ ;  $\mathbf{V}_S^k = \tau_S \mathbf{D}_S^k$ ;
5:    $\gamma = \frac{2}{k+2}$ ;
6:    $\mathbf{L}^{k+1} = \mathbf{L}^k + \gamma(\mathbf{V}_L^k - \mathbf{L}^k)$ ;
7:    $\mathbf{S}^{k+1} = \mathbf{S}^k + \gamma(\mathbf{V}_S^k - \mathbf{S}^k)$ ;
8: end for

```

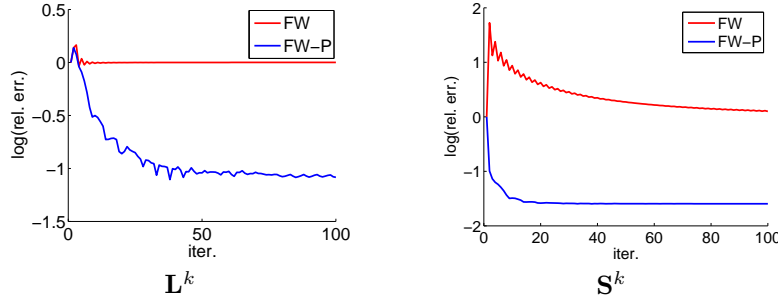


Figure 1: **Comparisons between Algorithm 3 and Algorithm 4 for problem (3.1) on synthetic data.** The data are generated in Matlab as $m = 1000$; $n = 1000$; $r = 5$; $\mathbf{L}_0 = \text{randn}(m, r) * \text{randn}(r, n)$; $\Omega = \text{ones}(m, n)$; $\mathbf{S}_0 = 100 * \text{randn}(m, n) .* (\text{rand}(m, n) < 0.01)$; $\mathbf{M} = \mathbf{L}_0 + \mathbf{S}_0 + \text{randn}(m, n)$; $\tau_L = \text{norm_nuc}(\mathbf{L}_0)$; $\tau_S = \text{norm}(\text{vec}(\mathbf{S}_0), 1)$; The left figure plots $\log_{10}(\|\mathbf{L}^k - \mathbf{L}_0\|_F / \|\mathbf{L}_0\|_F)$ versus the iteration number k . The right figure plots $\log_{10}(\|\mathbf{S}^k - \mathbf{S}_0\|_F / \|\mathbf{S}_0\|_F)$ versus k . The FW-P method is clearly more efficient than the straightforward FW method in recovering \mathbf{L}_0 and \mathbf{S}_0 .

3.2 FW-P algorithm: combining Frank-Wolfe and projected gradient

To overcome the drawback of the naive Frank-Wolfe algorithm, we propose to incorporate an additional gradient projection step after each Frank-Wolfe update. This additional step updates the sparse term \mathbf{S} only, with the goal of accelerating convergence in these variables. At iteration k , let $(\mathbf{L}^{k+1/2}, \mathbf{S}^{k+1/2})$ be the result produced by Frank-Wolfe. To produce the next iterate, we retain the low rank term $\mathbf{L}^{k+1/2}$, but set

$$\mathbf{S}^{k+1} = \mathcal{P}_{\|\cdot\|_1 \leq \tau_S} \left[\mathbf{S}^{k+\frac{1}{2}} - \nabla_{\mathbf{S}} l(\mathbf{L}^{k+\frac{1}{2}}, \mathbf{S}^{k+\frac{1}{2}}) \right] \quad (3.7)$$

$$= \mathcal{P}_{\|\cdot\|_1 \leq \tau_S} \left[\mathbf{S}^{k+\frac{1}{2}} - \mathcal{P}_Q[\mathbf{L}^{k+\frac{1}{2}} + \mathbf{S}^{k+\frac{1}{2}} - \mathbf{M}] \right]. \quad (3.8)$$

That is to say, we simply take an additional projected gradient step in the sparse term \mathbf{S} . We summarize the resulting algorithm as Algorithm 4. We call this method the FW-P algorithm, as it combines Frank-Wolfe steps and projections. In Figure 2, we compare Algorithms 3 and 4 on synthetic data. In this example, the FW-P method is clearly more efficient in recovering \mathbf{L}_0 and \mathbf{S}_0 .

The convergence of Algorithm 4 can be analyzed by recognizing it as a specific instance of the

Algorithm 4 FW-P method for problem (3.1)

```

1: Initialization:  $\mathbf{L}^0 = \mathbf{S}^0 = \mathbf{0}$ ;
2: for  $k = 0, 1, 2, \dots$  do
3:    $\mathbf{D}_L^k \in \arg \min_{\|\mathbf{D}_L\|_* \leq 1} \langle \mathcal{P}_Q[\mathbf{L}^k + \mathbf{S}^k - \mathbf{M}], \mathbf{D}_L \rangle$ ;  $\mathbf{V}_L^k = \tau_L \mathbf{D}_L^k$ ;
4:    $\mathbf{D}_S^k \in \arg \min_{\|\mathbf{D}_S\|_1 \leq 1} \langle \mathcal{P}_Q[\mathbf{L}^k + \mathbf{S}^k - \mathbf{M}], \mathbf{D}_S \rangle$ ;  $\mathbf{V}_S^k = \tau_S \mathbf{D}_S^k$ ;
5:    $\gamma = \frac{2}{k+2}$ ;
6:    $\mathbf{L}^{k+\frac{1}{2}} = \mathbf{L}^k + \gamma(\mathbf{V}_L^k - \mathbf{L}^k)$ ;
7:    $\mathbf{S}^{k+\frac{1}{2}} = \mathbf{S}^k + \gamma(\mathbf{V}_S^k - \mathbf{S}^k)$ ;
8:    $\mathbf{S}^{k+1} = \mathcal{P}_{\|\cdot\|_1 \leq \tau_S} [\mathbf{S}^{k+\frac{1}{2}} - \mathcal{P}_Q[\mathbf{L}^{k+\frac{1}{2}} + \mathbf{S}^{k+\frac{1}{2}} - \mathbf{M}]]$ ;
9:    $\mathbf{L}^{k+1} = \mathbf{L}^{k+\frac{1}{2}}$ ;
10: end for

```

generalized Frank-Wolfe iteration in Algorithm 2. This projection step (3.8) can be regarded as a proximal step to set \mathbf{S}^{k+1} as

$$\arg \min_{\|\mathbf{S}\|_1 \leq \tau_S} \hat{l}^{k+\frac{1}{2}}(\mathbf{S}) := l(\mathbf{L}^{k+\frac{1}{2}}, \mathbf{S}^{k+\frac{1}{2}}) + \langle \nabla_{\mathbf{S}} l(\mathbf{L}^{k+\frac{1}{2}}, \mathbf{S}^{k+\frac{1}{2}}), \mathbf{S} - \mathbf{S}^{k+\frac{1}{2}} \rangle + \frac{1}{2} \left\| \mathbf{S} - \mathbf{S}^{k+\frac{1}{2}} \right\|_F^2.$$

It can then be easily verified that $\hat{l}^{k+\frac{1}{2}}(\cdot)$ is a majorization function over $l(\mathbf{L}^{k+\frac{1}{2}}, \cdot)$ at point $\mathbf{S}^{k+\frac{1}{2}}$, i.e.,

$$\hat{l}^{k+\frac{1}{2}}(\mathbf{S}^{k+\frac{1}{2}}) = l(\mathbf{L}^{k+\frac{1}{2}}, \mathbf{S}^{k+\frac{1}{2}}), \quad \text{and} \quad \hat{l}^{k+\frac{1}{2}}(\mathbf{S}) \geq l(\mathbf{L}^{k+\frac{1}{2}}, \mathbf{S}) \quad \text{for any } \mathbf{S}. \quad (3.9)$$

This implies that the FW-P algorithm chooses a next iterate whose objective is no worse than that produced by the Frank-Wolfe step:

$$\begin{aligned} l(\mathbf{L}^{k+1}, \mathbf{S}^{k+1}) &\leq \hat{l}^{k+1/2}(\mathbf{S}^{k+1}) \\ &\leq \hat{l}^{k+1/2}(\mathbf{S}^{k+1/2}) \\ &\leq l(\mathbf{L}^{k+1/2}, \mathbf{S}^{k+1/2}). \end{aligned} \quad (3.10)$$

This is precisely the property that is required to invoke the more general analysis of Frank-Wolfe in Algorithm 2, Theorem 1 and Theorem 2. Using Lemmas 3 and 4 to estimate the Lipschitz constant of ∇l and the diameter of \mathcal{D} , we obtain the following result, which shows that FW-P retains the $O(1/k)$ convergence rate of the original FW method:

Theorem 3. *Let l^* be the optimal value to problem (3.1), $\mathbf{x}^k = (\mathbf{L}^k, \mathbf{S}^k)$ and $\mathbf{v}^k = (\mathbf{V}_L^k, \mathbf{V}_S^k)$ be the sequence produced by Algorithm 4. Then we have*

$$l(\mathbf{L}^k, \mathbf{S}^k) - l^* \leq \frac{16(\tau_L^2 + \tau_S^2)}{k+2}. \quad (3.11)$$

Moreover, for any $K \geq 1$, there exists $1 \leq \tilde{k} \leq K$ such that the surrogate duality gap (defined in (2.9)) satisfies

$$d(\mathbf{x}^{\tilde{k}}) = \left\langle \mathbf{x}^{\tilde{k}} - \mathbf{v}^{\tilde{k}}, \nabla l(\mathbf{x}^{\tilde{k}}) \right\rangle \leq \frac{48(\tau_L^2 + \tau_S^2)}{K+2}. \quad (3.12)$$

4 FW-T Method for Penalized Problem

In this section, we develop a scalable algorithm for the penalized version of the compressive principal component pursuit problem,

$$\min_{\mathbf{L}, \mathbf{S}} f(\mathbf{L}, \mathbf{S}) = \frac{1}{2} \|\mathcal{P}_Q[\mathbf{L} + \mathbf{S} - \mathbf{M}]\|_F^2 + \lambda_L \|\mathbf{L}\|_* + \lambda_S \|\mathbf{S}\|_1. \quad (4.1)$$

In Section 4.1, we reformulate problem (4.1) into the form of (2.1) so that Frank-Wolfe method can be applied. In Section 4.2, we apply Frank-Wolfe method directly to the reformulated problem, achieving linear per-iteration cost and $O(1/k)$ convergence in function value. However, because it updates the sparse term one element at a time, it converges very slowly on typical numerical examples. In Section 4, we introduce our FW-T method, which resolves this issue. Our FW-T method essentially exploits the Frank-Wolfe step to handle the nuclear norm and proximal gradient step to handle the ℓ_1 -norm, while retaining cheap iteration cost and convergence guarantees.

4.1 Reformulation as smooth, constrained optimization

Note that problem (4.1) has a non-differentiable objective function and an unbounded feasible set. To apply Frank-Wolfe method, we exploit a two-step reformulation to transform (4.1) into the form of (2.1). First, we borrow ideas from [HJN13] and work with the epigraph reformulation of (4.1),

$$\begin{aligned} \min \quad & g(\mathbf{L}, \mathbf{S}, t_L, t_S) \doteq \frac{1}{2} \|\mathcal{P}_Q[\mathbf{L} + \mathbf{S} - \mathbf{M}]\|_F^2 + \lambda_L t_L + \lambda_S t_S \\ \text{s.t.} \quad & \|\mathbf{L}\|_* \leq t_L, \quad \|\mathbf{S}\|_1 \leq t_S. \end{aligned} \quad (4.2)$$

Here, t_L and t_S are auxiliary variables of optimization. Now the objective function $g(\mathbf{L}, \mathbf{S}, t_L, t_S)$ is differentiable, with

$$\nabla_{\mathbf{L}} g(\mathbf{L}, \mathbf{S}, t_L, t_S) = \nabla_{\mathbf{S}} g(\mathbf{L}, \mathbf{S}, t_L, t_S) = \mathcal{P}_Q[\mathbf{L} + \mathbf{S} - \mathbf{M}], \quad (4.3)$$

$$\nabla_{t_L} g(\mathbf{L}, \mathbf{S}, t_L, t_S) = \lambda_L, \quad \nabla_{t_S} g(\mathbf{L}, \mathbf{S}, t_L, t_S) = \lambda_S. \quad (4.4)$$

A calculation, which we summarize as the following lemma, shows that the gradient $\nabla g(\mathbf{L}, \mathbf{S}, t_L, t_S) = (\nabla_{\mathbf{L}} g, \nabla_{\mathbf{S}} g, \nabla_{t_L} g, \nabla_{t_S} g)$ is 2-Lipschitz:

Lemma 3. *For all $(\mathbf{L}, \mathbf{S}, t_L, t_S)$ and $(\mathbf{L}', \mathbf{S}', t'_L, t'_S)$ feasible to (4.2),*

$$\|\nabla g(\mathbf{L}, \mathbf{S}, t_L, t_S) - \nabla g(\mathbf{L}', \mathbf{S}', t'_L, t'_S)\|_F \leq 2 \|(\mathbf{L}, \mathbf{S}, t_L, t_S) - (\mathbf{L}', \mathbf{S}', t'_L, t'_S)\|_F. \quad (4.5)$$

However, Frank-Wolfe method still cannot deal with (4.2), since its feasible region is unbounded. If we could somehow obtain bounds on the optimal values of t_L and t_S : $U_L \geq t_L^*$ and $U_S \geq t_S^*$, then we could solve the equivalent problem

$$\begin{aligned} \min \quad & \frac{1}{2} \|\mathcal{P}_Q[\mathbf{L} + \mathbf{S} - \mathbf{M}]\|_F^2 + \lambda_L t_L + \lambda_S t_S \\ \text{s.t.} \quad & \|\mathbf{L}\|_* \leq t_L \leq U_L, \quad \|\mathbf{S}\|_1 \leq t_S \leq U_S, \end{aligned} \quad (4.6)$$

which now has a compact and convex feasible set. One simple way to obtain such U_L, U_S is as follows. One trivial feasible solution for (4.2) is $\mathbf{L} = \mathbf{0}, \mathbf{S} = \mathbf{0}, t_L = 0, t_S = 0$. This solution has

objective value $\frac{1}{2} \|\mathcal{P}_Q[\mathbf{M}]\|_F^2$. Hence, the optimal objective value is no larger than this. This implies that for any optimal t_L^*, t_S^* ,

$$t_L^* \leq \frac{1}{2\lambda_L} \|\mathcal{P}_Q[\mathbf{M}]\|_F^2, \quad t_S^* \leq \frac{1}{2\lambda_S} \|\mathcal{P}_Q[\mathbf{M}]\|_F^2. \quad (4.7)$$

Hence, we can always choose

$$U_L = \frac{1}{2\lambda_L} \|\mathcal{P}_Q[\mathbf{M}]\|_F^2, \quad U_S = \frac{1}{2\lambda_S} \|\mathcal{P}_Q[\mathbf{M}]\|_F^2 \quad (4.8)$$

to produce a valid, bounded feasible region. The following lemma bounds its diameter D :

Lemma 4. *The feasible set $\mathcal{D} = \{(\mathbf{L}, \mathbf{S}, t_L, t_S) \mid \|\mathbf{L}\|_* \leq t_L \leq U_L, \|\mathbf{S}\|_1 \leq t_S \leq U_S\}$ has diameter $D \leq \sqrt{5} \cdot \sqrt{U_L^2 + U_S^2}$.*

With these modifications, we can apply Frank-Wolfe directly to obtain a solution $(\widehat{\mathbf{L}}, \widehat{\mathbf{S}}, \widehat{t}_L, \widehat{t}_S)$ to (4.6), and hence to produce a solution $(\widehat{\mathbf{L}}, \widehat{\mathbf{S}})$ to the original problem (4.1). In subsection 4.2, we describe how to do this. This straightforward solution will have two main disadvantages. First, similar to the norm constrained case, it produces only one-sparse updates to \mathbf{S} , which results in slow convergence. Second, the exact primal convergence rate in Theorem 1 depends on the diameter of the feasible set, which in turn depends on the accuracy of our (crude) upper bounds U_L and U_S . In subsection 4.3, we show how to remedy both issues, yielding Frank-Wolfe-Thresholding method with significantly better practical performance.

4.2 Frank-Wolfe for problem (4.6)

Applying Frank-Wolfe method in Algorithm 1 generates a sequence of iterates $\mathbf{x}^k = (\mathbf{L}^k, \mathbf{S}^k, t_L^k, t_S^k)$. Using the expressions for the gradient in (4.3) and (4.4), at each iteration, $\mathbf{v}^k = (\mathbf{V}_L^k, \mathbf{V}_S^k, V_{t_L}^k, V_{t_S}^k)$ is generated by solving the linearized subproblem

$$\mathbf{v}^k \in \arg \min_{\mathbf{v} \in \mathcal{D}} \langle \mathcal{P}_Q[\mathbf{L}^k + \mathbf{S}^k - \mathbf{M}], \mathbf{V}_L + \mathbf{V}_S \rangle + \lambda_L V_{t_L} + \lambda_S V_{t_S}, \quad (4.9)$$

which can be decoupled into two independent subproblems,

$$(\mathbf{V}_L^k, V_{t_L}^k) \in \arg \min_{\|\mathbf{V}_L\|_* \leq V_{t_L} \leq U_L} g_L(\mathbf{V}_L, V_{t_L}) \doteq \langle \mathcal{P}_Q[\mathbf{L}^k + \mathbf{S}^k - \mathbf{M}], \mathbf{V}_L \rangle + \lambda_L V_{t_L} \quad (4.10)$$

$$(\mathbf{V}_S^k, V_{t_S}^k) \in \arg \min_{\|\mathbf{V}_S\|_1 \leq V_{t_S} \leq U_S} g_S(\mathbf{V}_S, V_{t_S}) \doteq \langle \mathcal{P}_Q[\mathbf{L}^k + \mathbf{S}^k - \mathbf{M}], \mathbf{V}_S \rangle + \lambda_S V_{t_S}. \quad (4.11)$$

Let us consider problem (4.10) first. Set

$$\mathbf{D}_L^k \in \arg \min_{\|\mathbf{D}_L\|_* \leq 1} \hat{g}_L(\mathbf{D}_L) \doteq \langle \mathcal{P}_Q[\mathbf{L}^k + \mathbf{S}^k - \mathbf{M}], \mathbf{D}_L \rangle + \lambda_L. \quad (4.12)$$

Because $g_L(\mathbf{V}_L, V_{t_L})$ is a homogeneous function, i.e., $g_L(\alpha \mathbf{V}_L, \alpha V_{t_L}) = \alpha g_L(\mathbf{V}_L, V_{t_L})$, for any $\alpha \in \mathbb{R}$, its optimal value $g(\mathbf{V}_L^k, V_{t_L}^k) = V_{t_L}^k \hat{g}_L(\mathbf{D}_L^k)$. Hence $V_{t_L}^k = U_L$ if $\hat{g}_L(\mathbf{D}_L^k) < 0$, and $V_{t_L}^k = 0$ if $\hat{g}_L(\mathbf{D}_L^k) > 0$. By this observation, it can be easily verified (see also [HJN13, Lemma 1] for a more general result) that

$$(\mathbf{V}_L^k, V_{t_L}^k) \in \begin{cases} \{(\mathbf{0}, 0)\} & \text{if } \hat{g}_L(\mathbf{D}_L^k) > 0 \\ \text{conv}\{(\mathbf{0}, 0), U_L(\mathbf{D}_L^k, 1)\} & \text{if } \hat{g}_L(\mathbf{D}_L^k) = 0 \\ \{U_L(\mathbf{D}_L^k, 1)\} & \text{if } \hat{g}_L(\mathbf{D}_L^k) < 0. \end{cases} \quad (4.13)$$

Algorithm 5 Frank-Wolfe method for problem (4.6)

```

1: Initialization:  $\mathbf{L}^0 = \mathbf{S}^0 = \mathbf{0}$ ;  $t_L^0 = t_S^0 = 0$ ;
2: for  $k = 0, 1, 2, \dots$  do
3:    $\mathbf{D}_L^k \in \arg \min_{\|\mathbf{D}_L\|_* \leq 1} \langle \mathcal{P}_Q[\mathbf{L}^k + \mathbf{S}^k - \mathbf{M}], \mathbf{D}_L \rangle$ ;
4:    $\mathbf{D}_S^k \in \arg \min_{\|\mathbf{D}_S\|_1 \leq 1} \langle \mathcal{P}_Q[\mathbf{L}^k + \mathbf{S}^k - \mathbf{M}], \mathbf{D}_S \rangle$ ;
5:   if  $\lambda_L \geq -\langle \mathcal{P}_Q[\mathbf{L}^k + \mathbf{S}^k - \mathbf{M}], \mathbf{D}_L^k \rangle$  then
6:      $\mathbf{V}_L^k = \mathbf{0}$ ;  $V_{t_L}^k = 0$ 
7:   else
8:      $\mathbf{V}_L^k = U_L \mathbf{D}_L^k$ ,  $V_{t_L}^k = U_L$ ;
9:   end if
10:  if  $\lambda_S \geq -\langle \mathcal{P}_Q[\mathbf{L}^k + \mathbf{S}^k - \mathbf{M}], \mathbf{D}_S^k \rangle$  then
11:     $\mathbf{V}_S^k = \mathbf{0}$ ;  $V_{t_S}^k = 0$ ;
12:  else
13:     $\mathbf{V}_S^k = U_S \mathbf{D}_S^k$ ,  $V_{t_S}^k = U_S$ ;
14:  end if
15:   $\gamma = \frac{2}{k+2}$ ;
16:   $\mathbf{L}^{k+1} = (1 - \gamma)\mathbf{L}^k + \gamma\mathbf{V}_L^k$ ,  $t_L^{k+1} = (1 - \gamma)t_L^k + \gamma V_{t_L}^k$ ;
17:   $\mathbf{S}^{k+1} = (1 - \gamma)\mathbf{S}^k + \gamma\mathbf{V}_S^k$ ,  $t_S^{k+1} = (1 - \gamma)t_S^k + \gamma V_{t_S}^k$ ;
18: end for

```

In a similar manner, we can update $(\mathbf{V}_S^k, V_{t_S}^k)$. This leads fairly directly to an implementation of the Frank-Wolfe method for problem (4.6), which we describe in Algorithm 5. As a direct corollary of Theorem 1, using parameters calculated in Lemmas 3 and 4, we have

Corollary 4. *Let $\mathbf{x}^* = (\mathbf{L}^*, \mathbf{S}^*, t_L^*, t_S^*)$ be an optimal solution to (4.6). For $\{\mathbf{x}^k\}$ generated by Algorithm 5, we have³ for $k = 0, 1, 2, \dots$,*

$$g(\mathbf{x}^k) - g(\mathbf{x}^*) \leq \frac{20(U_L^2 + U_S^2)}{k+2}. \quad (4.14)$$

In addition to the above convergence result, another major advantage of Algorithm 5 derives from the simplicity of the update rules (lines 3-4 in Algorithm 5). Both have closed form solution and both can be computed in time (essentially) linearly dependent on the size of the input.

However, two clear limitations substantially hinder its efficiency. First, similar to the norm constrained case, as \mathbf{V}_S^k has only one nonzero entry, \mathbf{S} has a one-sparse update in each iteration, which is very inefficient. Another drawback of Algorithm 5 is that the exact rate of convergence relies on our (crude) guesses U_L and U_S (Corollary 4). The red curves in Figure 2 show these effects on the practical convergence of the algorithm, on a simulated example of size $1,000 \times 1,000$, in which about 1% of the entries in the target sparse matrix \mathbf{S}_0 are nonzero.⁴ As we can observe, progress is very slow. In the next part, we present remedies to resolve both issues.

³A more careful calculation would lead us to $g(\mathbf{x}^k) - g(\mathbf{x}^*) \leq \frac{16(U_L^2 + U_S^2)}{k+2}$, which we also include in the appendix.

⁴In specific, the data are generated in Matlab as $m = 1000$; $n = 1000$; $r = 5$; $L_0 = \text{randn}(m, r) * \text{randn}(r, n)$; $\text{Omega} = \text{ones}(m, n)$; $S_0 = 100 * \text{randn}(m, n) .* (\text{rand}(m, n) < 0.01)$; $M = L_0 + S_0 + 0.1 * \text{randn}(m, n)$;

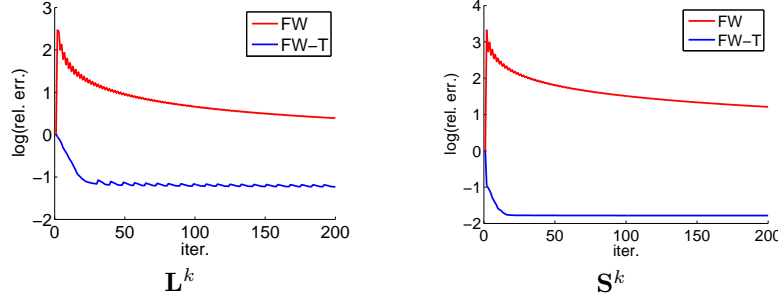


Figure 2: **Comparison between Algorithm 5 and Algorithm 6 for problem (4.6) on synthetic data.** We set weights $\lambda_L = 0.005 \|\mathbf{M}\|_F$, $\lambda_S = 0.005 \|\mathbf{M}\|_F / \sqrt{1000}$. The left figure plots $\log_{10}(\|\mathbf{L}^k - \mathbf{L}_0\|_F / \|\mathbf{L}_0\|_F)$ versus the iteration number k . The right figure plots $\log_{10}(\|\mathbf{S}^k - \mathbf{S}_0\|_F / \|\mathbf{S}_0\|_F)$ versus k . The FW-T method is clearly more efficient than the straightforward FW method in recovering \mathbf{L}_0 and \mathbf{S}_0 .

4.3 FW-T algorithm: combining Frank-Wolfe and proximal methods

To alleviate the difficulties faced by Algorithm 5, we design a new algorithm called Frank-Wolfe-Thresholding (FW-T) (Algorithm 6), which combines a modified FW step and a proximal gradient step. In Figure 2, we compare Algorithms 5 and 6 on synthetic data. In this example, the FW-T method is clearly more efficient in recovering \mathbf{L}_0 and \mathbf{S}_0 . Below we highlight key features in FW-T.

Proximal gradient step for \mathbf{S} . To update \mathbf{S} in a more efficient way, we incorporate an additional proximal gradient step for \mathbf{S} . At iteration k , let $(\mathbf{L}^{k+\frac{1}{2}}, \mathbf{S}^{k+\frac{1}{2}})$ be the result produced by Frank-Wolfe step. To produce the next iterate, we retain the low-rank term $\mathbf{L}^{k+\frac{1}{2}}$, but execute a proximal gradient step for function $f(\mathbf{L}^{k+\frac{1}{2}}, \mathbf{S})$ at the point $\mathbf{S}^{k+\frac{1}{2}}$, i.e.

$$\begin{aligned} \mathbf{S}^{k+1} &\in \arg \min_{\mathbf{S}} \left\langle \nabla_{\mathbf{S}} f(\mathbf{L}^{k+\frac{1}{2}}, \mathbf{S}^{k+\frac{1}{2}}), \mathbf{S} - \mathbf{S}^{k+\frac{1}{2}} \right\rangle + \frac{1}{2} \|\mathbf{S} - \mathbf{S}^{k+\frac{1}{2}}\|_F^2 + \lambda_S \|\mathbf{S}\|_1 \\ &= \arg \min_{\mathbf{S}} \left\langle \mathcal{P}_Q[\mathbf{L}^{k+\frac{1}{2}} + \mathbf{S}^{k+\frac{1}{2}} - \mathbf{M}], \mathbf{S} - \mathbf{S}^{k+\frac{1}{2}} \right\rangle + \frac{1}{2} \|\mathbf{S} - \mathbf{S}^{k+\frac{1}{2}}\|_F^2 + \lambda_S \|\mathbf{S}\|_1 \end{aligned} \quad (4.15)$$

which can be easily solved via the soft-thresholding operator:

$$\mathbf{S}^{k+1} = \mathcal{T} \left[\mathbf{S}^{k+\frac{1}{2}} - \mathcal{P}_\Omega[\mathbf{L}^{k+\frac{1}{2}} + \mathbf{S}^{k+\frac{1}{2}} - \mathbf{M}], \lambda_S \right]. \quad (4.16)$$

Exact line search. For the Frank-Wolfe step, instead of choosing the fixed step length $\frac{2}{k+2}$, we implement an exact line search by solving a two-dimensional quadratic problem (4.18), as in [HJN13]. This modification turns out to be crucial to achieve a primal convergence result that only weakly depends on the tightness of our guesses U_L and U_S .

Adaptive updates on U_L and U_S . We initialize U_L and U_S using the crude bound (4.8). Then, at the end of the k -iteration, we respectively update

$$U_L^{k+1} = g(\mathbf{L}^{k+1}, \mathbf{S}^{k+1}, t_L^{k+1}, t_S^{k+1}) / \lambda_L, \quad U_S^{k+1} = g(\mathbf{L}^{k+1}, \mathbf{S}^{k+1}, t_L^{k+1}, t_S^{k+1}) / \lambda_S. \quad (4.17)$$

Algorithm 6 FW-T method for problem (4.1)

- 1: **Input:** data matrix $\mathbf{M} \in \mathbb{R}^{m \times n}$; weights $\lambda_L, \lambda_S > 0$; max iteration number T ;
- 2: **Initialization:** $\mathbf{L}^0 = \mathbf{S}^0 = \mathbf{0}$; $t_L^0 = t_S^0 = 0$; $U_L^0 = g(\mathbf{L}^0, \mathbf{S}^0, t_L^0, t_S^0)/\lambda_L$; $U_S^0 = g(\mathbf{L}^0, \mathbf{S}^0, t_L^0, t_S^0)/\lambda_S$;
- 3: **for** $k = 0, 1, 2, \dots, T$ **do**
- 4: *same as lines 3-14 in Algorithm 5;*
- 5: $\left(\mathbf{L}^{k+\frac{1}{2}}, \mathbf{S}^{k+\frac{1}{2}}, t_L^{k+\frac{1}{2}}, t_S^{k+\frac{1}{2}} \right)$ is computed as an optimizer to

$$\begin{aligned} \min \quad & \frac{1}{2} \|\mathcal{P}_Q[\mathbf{L} + \mathbf{S} - \mathbf{M}]\|_F^2 + \lambda_L t_L + \lambda_S t_S \\ \text{s.t.} \quad & \begin{pmatrix} \mathbf{L} \\ t_L \end{pmatrix} \in \text{conv} \left\{ \begin{pmatrix} \mathbf{L}^k \\ t_L^k \end{pmatrix}, \begin{pmatrix} \mathbf{V}_L^k \\ V_{t_L}^k \end{pmatrix} \right\}, \begin{pmatrix} \mathbf{S} \\ t_S \end{pmatrix} \in \text{conv} \left\{ \begin{pmatrix} \mathbf{S}^k \\ t_S^k \end{pmatrix}, \begin{pmatrix} \mathbf{V}_S^k \\ V_{t_S}^k \end{pmatrix} \right\}; \end{aligned} \quad (4.18)$$

- 6: $\mathbf{S}^{k+1} = \mathcal{T}[\mathbf{S}^{k+\frac{1}{2}} - \mathcal{P}_Q[\mathbf{L}^{k+\frac{1}{2}} + \mathbf{S}^{k+\frac{1}{2}} - \mathbf{M}], \lambda_S]$;
 - 7: $\mathbf{L}^{k+1} = \mathbf{L}^{k+\frac{1}{2}}, t_L^{k+1} = t_L^{k+\frac{1}{2}}; t_S^{k+1} = \|\mathbf{S}^{k+1}\|_1$;
 - 8: $U_L^{k+1} = g(\mathbf{L}^{k+1}, \mathbf{S}^{k+1}, t_L^{k+1}, t_S^{k+1})/\lambda_L$;
 - 9: $U_S^{k+1} = g(\mathbf{L}^{k+1}, \mathbf{S}^{k+1}, t_L^{k+1}, t_S^{k+1})/\lambda_S$;
 - 10: **end for**
-

This scheme maintains the property that $U_L^{k+1} \geq t_L^*$ and $U_S^{k+1} \geq t_S^*$. Moreover, we will prove in (Lemma 5) that g is non-increasing through our algorithm, and so this scheme produces a sequence of tighter upper bounds for U_L^* and U_S^* . Although this dynamic scheme does not improve the theoretical convergence result, slight acceleration is empirically witnessed.

Convergence analysis. Since both the FW step and the proximal gradient step do not increase the objective value, we can easily recognize FW-T method as a descent algorithm:

Lemma 5. *Let $\{(\mathbf{L}^k, \mathbf{S}^k, t_L^k, t_S^k)\}$ be the sequence of iterates produced by the FW-T algorithm. For each $k = 0, 1, 2, \dots$,*

$$g(\mathbf{L}^{k+1}, \mathbf{S}^{k+1}, t_L^{k+1}, t_S^{k+1}) \leq g(\mathbf{L}^{k+\frac{1}{2}}, \mathbf{S}^{k+\frac{1}{2}}, t_L^{k+\frac{1}{2}}, t_S^{k+\frac{1}{2}}) \leq g(\mathbf{L}^k, \mathbf{S}^k, t_L^k, t_S^k). \quad (4.19)$$

Moreover, we can establish primal convergence (almost) independent of U_L^0 and U_S^0 :

Theorem 5. *Let r_L^* and r_S^* be the smallest radii such that*

$$\left\{ (\mathbf{L}, \mathbf{S}) \mid f(\mathbf{L}, \mathbf{S}) \leq g(\mathbf{L}^0, \mathbf{S}^0, t_L^0, t_S^0) = \frac{1}{2} \|\mathcal{P}_Q[\mathbf{M}]\|_F^2 \right\} \subseteq \overline{B(r_L^*)} \times \overline{B(r_S^*)}, \quad (4.20)$$

where $\overline{B(r)} \doteq \{\mathbf{X} \in \mathbb{R}^{m \times n} \mid \|\mathbf{X}\|_F \leq r\}$ for any $r \geq 0$.⁵ Then for the sequence $\{(\mathbf{L}^k, \mathbf{S}^k, t_L^k, t_S^k)\}$ generated by Algorithm 6, we have

$$g(\mathbf{L}^k, \mathbf{S}^k, t_L^k, t_S^k) - g(\mathbf{L}^*, \mathbf{S}^*, t_L^*, t_S^*) \leq \frac{\min\{4(t_L^* + r_L^*)^2 + 4(t_S^* + r_S^*)^2, 16(U_L^0)^2 + 16(U_S^0)^2\}}{k+2}. \quad (4.21)$$

⁵Since the objective function in problem (4.1) is coercive, i.e. $\lim_{k \rightarrow +\infty} f(\mathbf{L}^k, \mathbf{S}^k) = +\infty$ for any sequence $(\mathbf{L}^k, \mathbf{S}^k)$ such that $\lim_{k \rightarrow +\infty} \|(\mathbf{L}^k, \mathbf{S}^k)\|_F = +\infty$, clearly $r_L^* \geq 0$ and $r_S^* \geq 0$ exist.

Since U_L^0 and U_S^0 are quite crude upper bounds for t_L^* and t_S^* , $16(U_L^0)^2 + 16(U_S^0)^2$ could be much larger than $4(t_L^* + r_L^*)^2 + 4(t_S^* + r_S^*)^2$. Therefore, this primal convergence results depend on U_L^0 and U_S^0 in a very weak manner.

However, the convergence result of the surrogate duality gap $d(\mathbf{x}^k)$ still hinges upon the upper bounds:

Theorem 6. *Let \mathbf{x}^k denote $(\mathbf{L}^k, \mathbf{S}^k, t_L^k, t_S^k)$ generated by Algorithm 6. Then for any $K \geq 1$, there exists $1 \leq \tilde{k} \leq K$ such that*

$$g(\mathbf{x}^{\tilde{k}}) - g(\mathbf{x}^*) \leq d(\mathbf{x}^{\tilde{k}}) \leq \frac{48((U_L^0)^2 + (U_S^0)^2)}{K + 2}. \quad (4.22)$$

Stopping criterion. Compared to the convergence of $g(\mathbf{x}^k)$ (Theorem 5), the convergence result for $d(\mathbf{x}^k)$ can be much slower (Theorem 6). Therefore, here the surrogate duality gap $d(\cdot)$ is not that suitable to serve as stopping criterion. Our stopping criterion is designed primarily based on the decreases of the objective values. In specific, we terminate the algorithm if

$$(g(\mathbf{x}^{k+1}) - g(\mathbf{x}^k)) / g(\mathbf{x}^k) \leq \varepsilon, \quad (4.23)$$

for consecutive five iterations.

5 Numerical Experiments

In this section, we report numerical results obtained by applying our FW-T method (Algorithm 6) to problem (1.5) with real data arising from applications considered in [CLMW11]: foreground/background separation from surveillance videos, and shadow and specular removal from face images.

Given observations $\{\mathbf{M}_0(i, j) \mid (i, j) \in \Omega\}$ where $\Omega \subseteq \{1, \dots, m\} \times \{1, \dots, n\}$ is the index set of the observable entries in $\mathbf{M}_0 \in \mathbb{R}^{m \times n}$, we assigned weights

$$\lambda_L = \delta \rho \|\mathcal{P}_\Omega[\mathbf{M}_0]\|_F \quad \text{and} \quad \lambda_S = \delta \sqrt{\rho} \|\mathcal{P}_\Omega[\mathbf{M}_0]\|_F / \sqrt{\max(m, n)}$$

to problem (1.5),⁶ where $\rho = |\Omega|/mn$ and δ is chosen as 0.01 for most of our experiments. We compared our FW-T method with popular first-order methods ISTA and FISTA [BT09], both of which were implemented with partial SVD (see Appendix E). We set $\varepsilon = 10^{-3}$ in FW-T's stopping criterion,⁷ and terminated ISTA and FISTA whenever they reached the objective value returned by the FW-T method.⁸ All the experiments were conducted with Intel Xeon E5-2630 Processor (12 cores at 2.4 GHz), and 64GB RAM running MATLAB R2012b (64 bits).

Foreground-background separation from surveillance video. In surveillance videos, due to the strong correlation between frames, it is natural to model the background as low rank; while foreground objects, such as cars or pedestrians, normally occupy only a fraction of the video, can

⁶The ratio $\lambda_L/\lambda_S = \sqrt{\rho \max(m, n)}$ follows the suggestion in [CLMW11]. For applications in computer vision at least, our choices in λ_L and λ_S seem to be quite robust, although it is possible to improve the performance by making slight adjustments to our current settings of λ_L and λ_S .

⁷As discussed in [YZ11, YY13], with noisy data, solving optimization problem to very high accuracy does not necessarily improve the recovering quality. That is why we set ε to a modest accuracy.

⁸All codes are available at: <https://sites.google.com/site/mucun1988/publi>

Table 1: Comparisons of FW-T, ISTA and FISTA on surveillance video problems.

Video	m	n	ρ	δ	FW-T		ISTA		FISTA	
					iter.	cpu(s)	iter.	cpu	iter.	cpu
Lobby	20480	1000	0.5	0.01	9	21.04	54	280.5	21	196.6
Escalator	20800	3417	0.5	0.01	9	75.48	26	1518	16	1224
Mall	81920	1286	1.0	0.01	12	103.8	14	279.4	12	271.8
Penguin	786432	750	1.0	0.01	19	1047	25	3312	14	2383
Airport	25344	15730	1.0	0.001	122	4823	29	29641	14	16794
Square	19200	28181	1.0	0.001	175	9325	29	38182	13	18133

be treated as sparse. So, if we stack each frame as a column in the data matrix \mathbf{M}_0 , it is reasonable to assume $\mathbf{M}_0 \approx \mathbf{L}_0 + \mathbf{S}_0$, where \mathbf{L}_0 captures the background and \mathbf{S}_0 represents the foreground movements. Here, we solved problem (1.5) for videos introduced in [LHGT04] and [JRP07]. The observed entries were sampled uniformly with ratio ρ .

Table 5 summarizes the numerical performances of FW-T, ISTA and FISTA. Our FW-T method takes less time than ISTA and FISTA, and the advantage becomes more prominent as the size of data grows. In Figure 3, frames of the original videos, the backgrounds and the foregrounds produced by the FW-T method are presented, which are quite visually appealing.

Our FW-T method requires more iterations for large-scale videos (Airport, Square) than for medium-scale ones. This seems quite reasonable: as the number of frames grows, the background contains more variations, due to illumination changes, camera rotations, weather, etc., and so the rank increases⁹. Since our FW-T method only conducts a rank-one update on the low-rank component in each iteration, it requires more iterations to reach an accurate solution. However, because each iteration is significantly cheaper, the overall cost is still much less than that of ISTA and FISTA. To illustrate this more clearly, in Figure 4, we plot the per-iteration cost of these three methods on the Airport and Square videos with increasing number of frames. The computational cost of FW-T scales linearly with the size of the data, whereas the cost of the other methods increases superlinearly.

Shadow and specular removal from face images. Images taken under varying illumination can also be modeled as the superposition of low-rank and sparse components. Here, the data matrix \mathbf{M}_0 is again formed by stacking each image as a column. The low-rank term \mathbf{L}_0 captures the smooth variations [BJ03], while the sparse term \mathbf{S}_0 represents cast shadows and specularities [WYG⁺09, ZMKW13]. CPCP can be used to remove the shadows and specularities [CLMW11, ZMKW13]. Here, we solved problem (1.4) for Yale B face images [GBK01], and images rendered from 3D triangulated face models from [SSB12]. Full observations (i.e. $\rho = 1$) were assumed in this experiment. Table 2 summarizes the numerical performances of FW-T, ISTA and FISTA. Clearly, our FW-T method is more favorable for large-scale problems.

⁹That is also the reason why in these three videos we set δ smaller to reduce the weight for the nuclear norm and raise the weight for the data fidelity term.

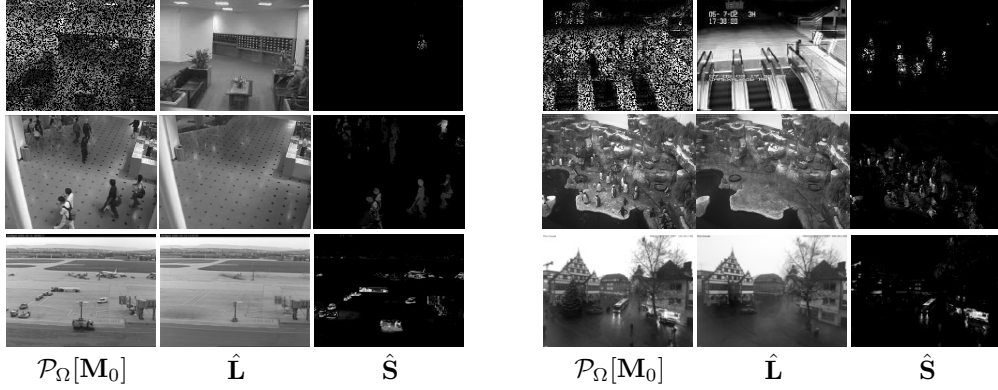


Figure 3: **Surveillance videos.** Visually, the low-rank component recovers the background and the sparse one captures the movements in the foreground.

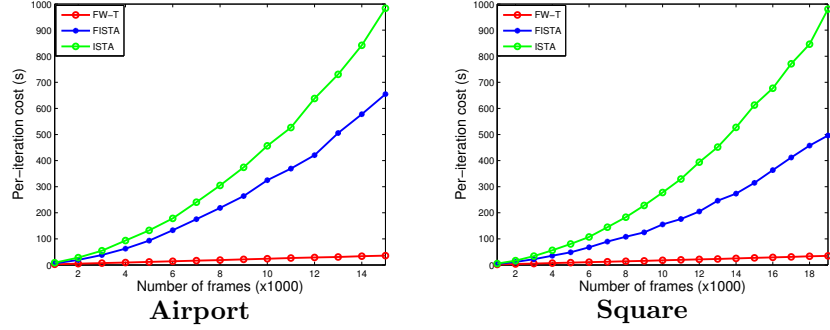


Figure 4: **Per-iteration cost vs. the number of frames in Airport and Square videos.** The per-iteration cost of our FW-T method grows linearly with the size of data, makes it more advantageous for large problems.

6 Conclusion

In this paper, we have proposed scalable algorithms called Frank-Wolfe-Projection (FW-P) and Frank-Wolfe-Thresholding (FW-T) for norm constrained and penalized versions of CPCP. Essentially, they combine classical ideas in Frank-Wolfe and Proximal methods to achieve linear per-iteration cost, $O(1/k)$ convergence in function value and practical efficiency in updating the sparse component. Promising numerical experiments have been conducted on computer vision related applications of CPCP, which demonstrate the great potentials of our methods in dealing with problems at large scale. It will be exciting to apply FW-P and FW-T to other CPCP applications, e.g., topic modelling [MZWM10] and dynamic MRI [OCS13].

Table 2: Comparisons of FW-T, ISTA and FISTA on face image problems.

Images	m	n	δ	FW-T		ISTA		FISTA	
				iter.	cpu(s)	iter.	cpu	iter.	cpu
YaleB01	32256	65	0.01	61	19.34	48	16.58	17	6.053
YaleB02	32256	65	0.01	62	20.66	51	17.18	18	6.036
Bosphorus000	40000	10000	0.001	166	5840	48	14328	21	6324
Bosphorus001	40000	10000	0.001	157	5601	55	16308	20	6384

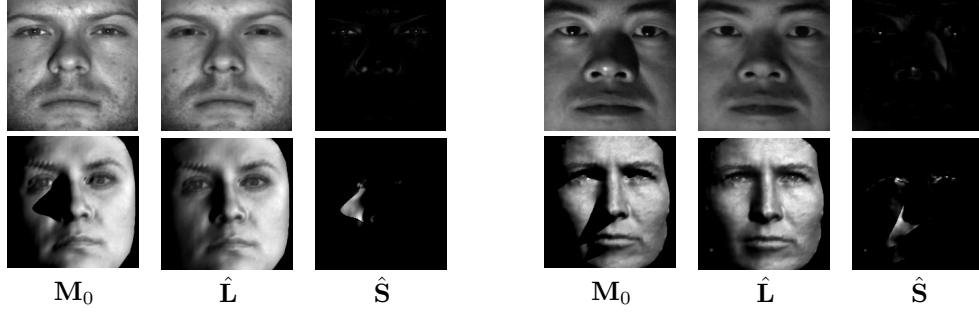


Figure 5: **Face images.** Visually, the recovered low-rank component is smoother and better conditioned for face recognition than the original image, while the sparse component corresponds to shadows and specularities.

Acknowledgment

It is a great pleasure to acknowledge conversations with Aleksandr Aravkin (IBM), Stephen Becker (IBM), Daniel Hsu (Columbia), Garud Iyengar (Columbia), Jianing Shi (UCLA), Waotao Yin (UCLA). CM was supported by the Class of 1988 Doctoral Fellowship. JW was supported by Columbia University startup funding and Office of Naval Research award N00014-13-1-0492. DG was supported by NSF Grant DMS-1016571.

References

- [AGI11] N. S. Aybat, D. Goldfarb, and G. Iyengar. Fast first-order methods for stable principal component pursuit. *arXiv preprint arXiv:1105.2126*, 2011.
- [AGM12] N. S. Aybat, D. Goldfarb, and S. Ma. Efficient algorithms for robust and stable principal component pursuit problems. *Computational Optimization and Applications*, pages 1–29, 2012.
- [ANW12] A. Agarwal, S. Negahban, and M. Wainwright. Noisy matrix decomposition via convex relaxation: Optimal rates in high dimensions. *The Annals of Statistics*, 40(2):1171–1197, 2012.
- [BJ03] R. Basri and D. Jacobs. Lambertian reflectance and linear subspaces. *IEEE Transactions on Pattern Analysis and Machine Intelligence*, 25(2):218–233, 2003.

- [BT09] A. Beck and M. Teboulle. A fast iterative shrinkage-thresholding algorithm for linear inverse problems. *SIAM Journal on Imaging Sciences*, 2(1):183–202, 2009.
- [CCS10] J. Cai, E. Candès, and Z. Shen. A singular value thresholding algorithm for matrix completion. *SIAM Journal on Optimization*, 20(4):1956–1982, 2010.
- [Cla10] K. Clarkson. Coresets, sparse greedy approximation, and the frank-wolfe algorithm. *ACM Trans. Algorithms*, 6(4):63:1–63:30, 2010.
- [CLMW11] E. Candès, X. Li, Y. Ma, and J. Wright. Robust principal component analysis? *Journal of the ACM (JACM)*, 58(3):11:1–11:37, 2011.
- [CPW12] V. Chandrasekaran, P. Parrilo, and A. Willsky. Latent variable graphical model selection via convex optimization. *Annals of Statistics*, 40(4):1935–1967, 2012.
- [CSPW11] V. Chandrasekaran, S. Sanghavi, P. Parrilo, and A. Willsky. Rank-sparsity incoherence for matrix decomposition. *SIAM Journal on Optimization*, 21(2):572–596, 2011.
- [DH78] J. C. Dunn and S. Harshbarger. Conditional gradient algorithms with open loop step size rules. *Journal of Mathematical Analysis and Applications*, 62(2):432 – 444, 1978.
- [DR70] V. F. Demianov and A. M. Rubinov. *Approximate methods in optimization problems*. Modern analytic and computational methods in science and mathematics. American Elsevier Pub. Co., 1970.
- [DSSSC08] J. Duchi, S. Shalev-Shwartz, Y. Singer, and T. Chandra. Efficient projections onto the l_1 -ball for learning in high dimensions. In *International Conference on Machine Learning (ICML)*, 2008.
- [FW56] M. Frank and P. Wolfe. An algorithm for quadratic programming. *Naval Research Logistics Quarterly*, 3(1-2):95–110, 1956.
- [GBK01] A. Georgiades, P. Belhumeur, and D. Kriegman. From few to many: Illumination cone models for face recognition under variable lighting and pose. *IEEE Transactions on Pattern Analysis and Machine Intelligence*, 23(6):643–660, 2001.
- [HJN13] Z. Harchaoui, A. Juditsky, and A. Nemirovski. Conditional gradient algorithms for norm-regularized smooth convex optimization. *arXiv preprint arXiv:1302.2325*, 2013.
- [HKZ11] D. Hsu, S. Kakade, and T. Zhang. Robust matrix decomposition with sparse corruptions. *IEEE Transactions on Information Theory*, 57(11):7221–7234, 2011.
- [Jag13] M. Jaggi. Revisiting frank-wolfe: Projection-free sparse convex optimization. In *International Conference on Machine Learning (ICML)*, 2013.
- [JRP07] N. Jacobs, N. Roman, and R. Pless. Consistent temporal variations in many outdoor scenes. In *Computer Vision and Pattern Recognition (CVPR)*, 2007.
- [JS10] M. Jaggi and M. Sulovsk. A simple algorithm for nuclear norm regularized problems. In *International Conference on Machine Learning (ICML)*, 2010.

- [LCM10] Z. Lin, M. Chen, and Y. Ma. The augmented lagrange multiplier method for exact recovery of corrupted low-rank matrices. *arXiv preprint arXiv:1009.5055*, 2010.
- [LGW⁺09] Z. Lin, A. Ganesh, J. Wright, L. Wu, M. Chen, and Y. Ma. Fast convex optimization algorithms for exact recovery of a corrupted low-rank matrix. *Computational Advances in Multi-Sensor Adaptive Processing (CAMSAP)*, 61, 2009.
- [LHGT04] L. Li, W. Huang, I. Y. Gu, and Q. Tian. Statistical modeling of complex backgrounds for foreground object detection. *IEEE Transactions on Image Processing*, 13(11):1459–1472, 2004.
- [LP66] E. Levitin and B. Polyak. Constrained minimization methods. *USSR Computational Mathematics and Mathematical Physics*, 6(5):1–50, 1966.
- [MGC11] S. Ma, D. Goldfarb, and L. Chen. Fixed point and bregman iterative methods for matrix rank minimization. *Mathematical Programming*, 128(1-2):321–353, 2011.
- [MZWM10] K. Min, Z. Zhang, J. Wright, and Y. Ma. Decomposing background topics from keywords by principal component pursuit. pages 269–278, 2010.
- [Nes83] Y. Nesterov. A method of solving a convex programming problem with convergence rate $o(1/k^2)$. In *Soviet Mathematics Doklady*, volume 27, pages 372–376, 1983.
- [OCS13] R. Otazo, E. Candès, and D. Sodickson. Low-rank and sparse matrix decomposition for accelerated dynamic mri with separation of background and dynamic components. *preprint*, 2013.
- [Pat93] M. Patriksson. Partial linearization methods in nonlinear programming. *Journal of Optimization Theory and Applications*, 78(2):227–246, 1993.
- [PGW⁺12] Y. Peng, A. Ganesh, J. Wright, W. Xu, and Y. Ma. Rasl: Robust alignment by sparse and low-rank decomposition for linearly correlated images. *IEEE Transactions on Pattern Analysis and Machine Intelligence*, 34(11):2233–2246, 2012.
- [SSB12] A. Savran, B. Sankur, and M. T. Bilge. Comparative evaluation of 3d vs. 2d modality for automatic detection of facial action units. *Pattern Recognition*, 45(2):767–782, 2012.
- [TTT03] R. Tütüncü, K. Toh, and M. Todd. Solving semidefinite-quadratic-linear programs using sdpt3. *Mathematical Programming*, 95(2):189–217, 2003.
- [TY11] M. Tao and X. Yuan. Recovering low-rank and sparse components of matrices from incomplete and noisy observations. *SIAM Journal on Optimization*, 21(1):57–81, 2011.
- [WGMM13] J. Wright, A. Ganesh, K. Min, and Y. Ma. Compressive principal component pursuit. *Information and Inference*, 2(1):32–68, 2013.
- [WGS⁺11] L. Wu, A. Ganesh, B. Shi, Y. Matsushita, Y. Wang, and Y. Ma. Robust photometric stereo via low-rank matrix completion and recovery. In *Asian Conference on Computer Vision (ACCV)*, 2011.

- [WYG⁺09] J. Wright, A. Yang, A. Ganesh, S. Sastry, and Y. Ma. Robust face recognition via sparse representation. *IEEE Transactions on Pattern Analysis and Machine Intelligence*, 31(2):210–227, 2009.
- [YY09] X. Yuan and J. Yang. Sparse and low-rank matrix decomposition via alternating direction methods. *preprint*, 2009.
- [YY13] J. Yang and X. Yuan. Linearized augmented lagrangian and alternating direction methods for nuclear norm minimization. *Mathematics of Computation*, 82(281):301–329, 2013.
- [YZ11] J. Yang and Y. Zhang. Alternating direction algorithms for ℓ_1 -problems in compressive sensing. *SIAM Journal on Scientific Computing*, 33(1):250–278, 2011.
- [Zha03] T. Zhang. Sequential greedy approximation for certain convex optimization problems. *Transactions on Information Theory*, 49(3):682–691, 2003.
- [ZLW⁺10] Z. Zhou, X. Li, J. Wright, E. Candes, and Y. Ma. Stable principal component pursuit. In *IEEE International Symposium on Information Theory Proceedings (ISIT)*, 2010.
- [ZMKW13] Y. Zhang, C. Mu, H. Kuo, and J. Wright. Towards guaranteed illumination models for nonconvex objects. In *International Conference on Computer Vision (ICCV)*, 2013.

A A Useful Recurrence

We first present an elementary but useful fact on real sequences, which is exploited quite frequently in the convergence proofs for FW-type algorithms.

Lemma A.1. *Consider a real sequence $\{a^k\}$. Suppose $\{a^k\}$ satisfies the following recursive relation:*

$$a^{k+1} \leq \frac{k}{k+2}a^k + \left(\frac{2}{k+2}\right)^2 C, \quad \text{for } k = 0, 1, 2, \dots, \quad (\text{A.1})$$

where C is a constant. Then for any $k = 1, 2, 3, \dots$, we have $a^k \leq \frac{4C}{k+2}$, and hence $\lim_{k \rightarrow \infty} a^k = 0$.

Proof. The proof is by induction. Clearly, from (A.1), we have $a^1 \leq C \leq \frac{4C}{1+2}$ as the base case. For any fixed $k \geq 1$, assume that $a^k \leq \frac{4C}{k+2}$. Then by (A.1),

$$a^{k+1} \leq \frac{k}{k+2}a^k + \left(\frac{2}{k+2}\right)^2 C \leq \frac{k}{k+2} \cdot \frac{4C}{k+2} + \frac{4C}{(k+2)^2} \quad (\text{A.2})$$

$$\leq \frac{4C(k+1)}{(k+2)^2} \leq \frac{4C(k+2)}{(k+2)(k+3)} = \frac{4C}{k+3}. \quad (\text{A.3})$$

Therefore, by induction, we have proved the claim. \square

B Proofs from Section 2

B.1 Proof of Theorem 1

Proof. For $k = 0, 1, 2, \dots$, we have

$$\begin{aligned} h(\mathbf{x}^{k+1}) &\leq h(\mathbf{x}^k + \gamma(\mathbf{v}^k - \mathbf{x}^k)) \\ &\leq h(\mathbf{x}^k) + \gamma \langle \nabla h(\mathbf{x}^k), \mathbf{v}^k - \mathbf{x}^k \rangle + \frac{L\gamma^2}{2} \|\mathbf{v}^k - \mathbf{x}^k\|^2 \\ &\leq h(\mathbf{x}^k) + \gamma \langle \nabla h(\mathbf{x}^k), \mathbf{v}^k - \mathbf{x}^k \rangle + \frac{\gamma^2 LD^2}{2} \end{aligned} \quad (\text{B.1})$$

$$\begin{aligned} &\leq h(\mathbf{x}^k) + \gamma \langle \nabla h(\mathbf{x}^k), \mathbf{x}^* - \mathbf{x}^k \rangle + \frac{\gamma^2 LD^2}{2} \\ &\leq h(\mathbf{x}^k) + \gamma(h(\mathbf{x}^*) - h(\mathbf{x}^k)) + \frac{\gamma^2 LD^2}{2}, \end{aligned} \quad (\text{B.2})$$

where the second inequality holds as $\nabla h(\cdot)$ is L -Lipschitz continuous; the third line follows because D is the diameter for the feasible set \mathcal{D} ; the fourth inequality follows from $\mathbf{v}^k \in \operatorname{argmin}_{\mathbf{v} \in \mathcal{D}} \langle \mathbf{v}, \nabla h(\mathbf{x}^k) \rangle$ and $\mathbf{x}^* \in \mathcal{D}$; the last one holds as $h(\cdot)$ is convex.

Rearranging terms in (B.2), one obtains that for $k = 0, 1, 2, \dots$,

$$h(\mathbf{x}^{k+1}) - h(\mathbf{x}^*) \leq (1 - \gamma) (h(\mathbf{x}^k) - h(\mathbf{x}^*)) + \frac{\gamma^2 LD^2}{2}. \quad (\text{B.3})$$

Therefore, by Lemma A.1,

$$h(\mathbf{x}^k) - h(\mathbf{x}^*) \leq \frac{2LD^2}{k+2}, \quad \text{for } k = 1, 2, 3, \dots$$

□

B.2 Proof of Theorem 2

Proof. For notational convenience, we denote $h^k \doteq h(\mathbf{x}^k)$, $\Delta^k \doteq h(\mathbf{x}^k) - h(\mathbf{x}^*)$, $d^k \doteq d(\mathbf{x}^k)$, $C \doteq 2LD^2$, $B \doteq K + 2$, $\hat{k} \doteq \lceil \frac{1}{2}B \rceil - 1$, $\mu \doteq \lceil \frac{1}{2}B \rceil / B$.

Suppose on the contrary that

$$d^k > \frac{3C}{B}, \quad \text{for all } k \in \left\{ \lceil \frac{1}{2}B \rceil - 1, \lceil \frac{1}{2}B \rceil, \dots, K \right\}. \quad (\text{B.4})$$

From (B.1), we know that for any $k \geq 1$

$$\Delta^{k+1} \leq \Delta^k + \gamma \langle \nabla h(\mathbf{x}^k), \mathbf{v}^k - \mathbf{x}^k \rangle + \frac{\gamma^2 LD^2}{2} = \Delta^k - \frac{2d^k}{k+2} + \frac{C}{(k+2)^2}. \quad (\text{B.5})$$

Therefore, by using (B.5) repeatedly, one has

$$\begin{aligned}
\Delta^{K+1} &\leq \Delta^{\hat{k}} - \sum_{k=\hat{k}}^K \frac{2d^k}{k+2} + \sum_{k=\hat{k}}^K \frac{C}{(k+2)^2} \\
&< \Delta^{\hat{k}} - \frac{6C}{B} \sum_{k=\hat{k}}^K \frac{1}{k+2} + C \sum_{k=\hat{k}}^K \frac{1}{(k+2)^2} \\
&= \Delta^{\hat{k}} - \frac{6C}{B} \sum_{k=\hat{k}+2}^B \frac{1}{k} + C \sum_{k=\hat{k}+2}^B \frac{1}{k^2} \\
&\leq \frac{C}{\mu B} - \frac{6C}{B} \cdot \frac{B - \hat{k} - 1}{B} + C \cdot \frac{B - \hat{k} - 1}{B(\hat{k} + 1)} \\
&= \frac{C}{\mu B} - \frac{6C}{B}(1 - \mu) + \frac{C}{B} \frac{1 - \mu}{\mu} \\
&= \frac{C}{\mu B} (2 - 6\mu(1 - \mu) - \mu)
\end{aligned} \tag{B.6}$$

where the second line is due to our assumption (B.4); the fourth line holds as $\Delta^{\hat{k}} \leq \frac{C}{\hat{k}+2}$ by Theorem 1, and $\sum_{k=a}^b \frac{1}{k^2} \leq \frac{b-a+1}{b(a-1)}$ for any $b \geq a > 1$.

Now define $\phi(x) = 2 - 6x(1 - x) - x$. Clearly $\phi(\cdot)$ is convex. Since $\phi(\frac{1}{2}) = \phi(\frac{2}{3}) = 0$, we have $\phi(x) \leq 0$ for any $x \in [\frac{1}{2}, \frac{2}{3}]$. As $\mu = \lceil \frac{1}{2}B \rceil / B \in [\frac{1}{2}, \frac{2}{3}]$, from (B.6), we have

$$\Delta^{K+1} = h(\mathbf{x}^{K+1}) - h(\mathbf{x}^*) < \frac{C}{\mu B} \phi(\mu) \leq 0,$$

which is a contradiction. \square

C Proofs from Section 3

C.1 Proof of Lemma 1

Proof. We calculate:

$$\begin{aligned}
\|\nabla l(\mathbf{L}, \mathbf{S}) - \nabla l(\mathbf{L}', \mathbf{S}')\|_F^2 &= 2 \|\mathcal{P}_Q[\mathbf{L} + \mathbf{S} - \mathbf{M}] - \mathcal{P}_Q[\mathbf{L}' + \mathbf{S}' - \mathbf{M}]\|_F^2 \\
&= 2 \|\mathcal{P}_Q[\mathbf{L} + \mathbf{S}] - \mathcal{P}_Q[\mathbf{L}' + \mathbf{S}']\|_F^2 \\
&\leq 2 \|\mathbf{L} + \mathbf{S} - \mathbf{L}' - \mathbf{S}'\|_F^2 \\
&\leq 4 \|\mathbf{L} - \mathbf{L}'\|_F^2 + 4 \|\mathbf{S} - \mathbf{S}'\|_F^2 \\
&= 4 \|(\mathbf{L}, \mathbf{S}) - (\mathbf{L}', \mathbf{S}')\|_F^2.
\end{aligned}$$

\square

C.2 Proof of Lemma 2

Proof. Since for any $\mathbf{Z} = (\mathbf{L}, \mathbf{S})$ and $\mathbf{Z}' = (\mathbf{L}', \mathbf{S}') \in \mathcal{D}$,

$$\begin{aligned}\|\mathbf{Z} - \mathbf{Z}'\|_F^2 &= \|\mathbf{L} - \mathbf{L}'\|_F^2 + \|\mathbf{S} - \mathbf{S}'\|_F^2 \leq (\|\mathbf{L}\|_F + \|\mathbf{L}'\|_F)^2 + (\|\mathbf{S}\|_F + \|\mathbf{S}'\|_F)^2 \\ &\leq (\|\mathbf{L}\|_* + \|\mathbf{L}'\|_*)^2 + (\|\mathbf{S}\|_1 + \|\mathbf{S}'\|_1)^2 \leq 4\tau_L^2 + 4\tau_S^2.\end{aligned}\tag{C.1}$$

□

C.3 Proof of Theorem 3

Proof. Substituting $L = 2$ (Lemma 1) and $D \leq 2\sqrt{\tau_L^2 + \tau_S^2}$ (Lemma 2) into Theorem 1 and Theorem 2, we can easily obtain the results. □

D Proofs from Section 4

D.1 Proof of Lemma 3

Proof. We calculate:

$$\begin{aligned}& \|\nabla g(\mathbf{L}, \mathbf{S}, t_L, t_S) - \nabla g(\mathbf{L}', \mathbf{S}', t'_L, t'_S)\|_F^2 \\ &= 2\|\mathcal{P}_Q[\mathbf{L} + \mathbf{S} - \mathbf{M}] - \mathcal{P}_Q[\mathbf{L}' + \mathbf{S}' - \mathbf{M}]\|_F^2 + (\lambda_L - \lambda'_L)^2 + (\lambda_S - \lambda'_S)^2 \\ &= 2\|\mathcal{P}_Q[\mathbf{L} + \mathbf{S} - \mathbf{M}] - \mathcal{P}_Q[\mathbf{L}' + \mathbf{S}' - \mathbf{M}]\|_F^2 \\ &= 2\|\mathcal{P}_Q[\mathbf{L} + \mathbf{S}] - \mathcal{P}_Q[\mathbf{L}' + \mathbf{S}']\|_F^2 \\ &\leq 2\|\mathbf{L} + \mathbf{S} - \mathbf{L}' - \mathbf{S}'\|_F^2 \\ &\leq 4\|\mathbf{L} - \mathbf{L}'\|_F^2 + 4\|\mathbf{S} - \mathbf{S}'\|_F^2 \\ &\leq 4\|(\mathbf{L}, \mathbf{S}, t_L, t_S) - (\mathbf{L}', \mathbf{S}', t'_L, t'_S)\|_F^2,\end{aligned}$$

which implies the result. □

D.2 Proof of Lemma 4

Proof. Since for any $\mathbf{Z} = (\mathbf{L}, \mathbf{S}, t_L, t_S)$, $\mathbf{Z}' = (\mathbf{L}', \mathbf{S}', t'_L, t'_S) \in \mathcal{D}$, we have

$$\begin{aligned}\|\mathbf{Z} - \mathbf{Z}'\|_F^2 &= \|\mathbf{L} - \mathbf{L}'\|_F^2 + \|\mathbf{S} - \mathbf{S}'\|_F^2 + (t_L - t'_L)^2 + (t_S - t'_S)^2 \\ &\leq (\|\mathbf{L}\|_F + \|\mathbf{L}'\|_F)^2 + (\|\mathbf{S}\|_F + \|\mathbf{S}'\|_F)^2 + (t_L - t'_L)^2 + (t_S - t'_S)^2 \\ &\leq (\|\mathbf{L}\|_* + \|\mathbf{L}'\|_*)^2 + (\|\mathbf{S}\|_1 + \|\mathbf{S}'\|_1)^2 + (t_L - t'_L)^2 + (t_S - t'_S)^2 \\ &\leq (U_L + U_L)^2 + (U_S + U_S)^2 + U_L^2 + U_S^2 \\ &= 5(U_L^2 + U_S^2),\end{aligned}$$

which implies the result. □

D.3 Proof of Corollary 4

Proof. Applying Theorem 1 with parameters calculated in Lemmas 3 and 4, we directly have

$$g(\mathbf{x}^k) - g(\mathbf{x}^*) \leq \frac{2 \cdot 2 \cdot \left(\sqrt{5(U_L^2 + U_S^2)} \right)^2}{k+2} = \frac{20(U_L^2 + U_S^2)}{k+2}. \quad (\text{D.1})$$

A more careful calculation below slightly improves the constant in (D.1).

$$\begin{aligned} g(\mathbf{x}^{k+1}) &= g(\mathbf{x}^k + \gamma(\mathbf{v}^k - \mathbf{x}^k)) \\ &\leq g(\mathbf{x}^k) + \gamma \langle \nabla g(\mathbf{x}^k), \mathbf{v}^k - \mathbf{x}^k \rangle + \gamma^2 \|\mathbf{V}_L^k - \mathbf{L}^k\|_F^2 + \gamma^2 \|\mathbf{V}_S^k - \mathbf{S}^k\|_F^2 \\ &\leq g(\mathbf{x}^k) + \gamma \langle \nabla g(\mathbf{x}^k), \mathbf{v}^k - \mathbf{x}^k \rangle + 4\gamma^2(U_L^2 + U_S^2), \end{aligned} \quad (\text{D.2})$$

where the second line holds by noting that g is only linear in t_L and t_S ; the last line holds as

$$\begin{aligned} \|\mathbf{V}_L^k - \mathbf{L}^k\|_F^2 &\leq (\|\mathbf{V}_L^k\|_F + \|\mathbf{L}^k\|_F)^2 \leq (U_L + U_L)^2 = 4U_L^2, \quad \text{and} \\ \|\mathbf{V}_S^k - \mathbf{S}^k\|_F^2 &\leq (\|\mathbf{V}_S^k\|_F + \|\mathbf{S}^k\|_F)^2 \leq (U_S + U_S)^2 = 4U_S^2. \end{aligned}$$

Following the arguments in the proof of Theorem 1 with (B.1) replaced by (D.2), we can easily obtain that

$$g(\mathbf{x}^k) - g(\mathbf{x}^*) \leq \frac{16(U_L^2 + U_S^2)}{k+2}.$$

□

D.4 Proof of Lemma 5

Proof. Since $(\mathbf{L}^k, \mathbf{S}^k, t_L^k, t_S^k)$ is always feasible to the quadratic program (4.18),

$$g(\mathbf{L}^{k+\frac{1}{2}}, \mathbf{S}^{k+\frac{1}{2}}, t_L^{k+\frac{1}{2}}, t_S^{k+\frac{1}{2}}) \leq g(\mathbf{L}^k, \mathbf{S}^k, t_L^k, t_S^k). \quad (\text{D.3})$$

Based on (4.15), the threshold step (line 6 in Algorithm 3) can be written as

$$\begin{aligned} \mathbf{S}^{k+1} = \arg \min_{\mathbf{S}} \quad & \hat{g}^{k+\frac{1}{2}}(\mathbf{S}) \doteq \frac{1}{2} \left\| \mathcal{P}_Q[\mathbf{L}^{k+\frac{1}{2}} + \mathbf{S}^{k+\frac{1}{2}} - \mathbf{M}] \right\|_F^2 + \lambda_L t_L^{k+\frac{1}{2}} + \lambda_S \|\mathbf{S}\|_1 + \\ & \langle \mathcal{P}_Q[\mathbf{L}^{k+\frac{1}{2}} + \mathbf{S}^{k+\frac{1}{2}} - \mathbf{M}], \mathbf{S} - \mathbf{S}^{k+\frac{1}{2}} \rangle + \frac{1}{2} \left\| \mathbf{S} - \mathbf{S}^{k+\frac{1}{2}} \right\|_F^2. \end{aligned}$$

The following properties of $\hat{g}^{k+\frac{1}{2}}(\cdot)$ can be easily verified

$$\begin{aligned} \hat{g}^{k+\frac{1}{2}}(\mathbf{S}^{k+\frac{1}{2}}) &= g(\mathbf{L}^{k+\frac{1}{2}}, \mathbf{S}^{k+\frac{1}{2}}, t_L^{k+\frac{1}{2}}, \|\mathbf{S}^{k+\frac{1}{2}}\|_1) \leq g(\mathbf{L}^{k+\frac{1}{2}}, \mathbf{S}^{k+\frac{1}{2}}, t_L^{k+\frac{1}{2}}, t_S^{k+\frac{1}{2}}); \\ \hat{g}^{k+\frac{1}{2}}(\mathbf{S}) &\geq g(\mathbf{L}^{k+\frac{1}{2}}, \mathbf{S}, t_L^{k+\frac{1}{2}}, \|\mathbf{S}\|_1), \quad \text{for any } \mathbf{S}. \end{aligned}$$

Therefore, we have

$$\begin{aligned} g(\mathbf{L}^{k+1}, \mathbf{S}^{k+1}, t_L^{k+1}, t_S^{k+1}) &= g(\mathbf{L}^{k+\frac{1}{2}}, \mathbf{S}^{k+1}, t_L^{k+\frac{1}{2}}, t_S^{k+1}) \leq \hat{g}^{k+\frac{1}{2}}(\mathbf{S}^{k+1}) \\ &\leq \hat{g}^{k+\frac{1}{2}}(\mathbf{S}^{k+\frac{1}{2}}) \leq g(\mathbf{L}^{k+\frac{1}{2}}, \mathbf{S}^{k+\frac{1}{2}}, t_L^{k+\frac{1}{2}}, t_S^{k+\frac{1}{2}}) \end{aligned} \quad (\text{D.4})$$

Combining (D.3) and (D.4), we obtain

$$g(\mathbf{L}^{k+1}, \mathbf{S}^{k+1}, t_L^{k+1}, t_S^{k+1}) \leq g(\mathbf{L}^{k+\frac{1}{2}}, \mathbf{S}^{k+\frac{1}{2}}, t_L^{k+\frac{1}{2}}, t_S^{k+\frac{1}{2}}) \leq g(\mathbf{L}^k, \mathbf{S}^k, t_L^k, t_S^k).$$

□

D.5 Proof of Theorem 5

For notational convenience, we denote

$$\mathbf{x}^k = (\mathbf{L}^k, \mathbf{S}^k, t_L^k, t_S^k), \mathbf{x}^* = (\mathbf{L}^*, \mathbf{S}^*, t_L^*, t_S^*) \text{ and } \mathbf{v}^k = (\mathbf{V}_L^k, \mathbf{V}_S^k, \mathbf{V}_{t_L}^k, \mathbf{V}_{t_S}^k).$$

For any point $\mathbf{x} = (\mathbf{L}, \mathbf{S}, t_L, t_S) \in \mathbb{R}^{m \times n} \times \mathbb{R}^{m \times n} \times \mathbb{R} \times \mathbb{R}$, we adopt the notation that $\mathbf{L}[\mathbf{x}] = \mathbf{L}$, $\mathbf{S}[\mathbf{x}] = \mathbf{S}$, $t_L[\mathbf{x}] = t_L$ and $t_S[\mathbf{x}] = t_S$.

Since $g(\mathbf{x}^k) - g(\mathbf{x}^*) \leq \frac{16(U_L^0)^2 + 16(U_S^0)^2}{k+2}$ can be easily established following the proof of Corollary 4, below we will focus on the proof of $g(\mathbf{x}^k) - g(\mathbf{x}^*) \leq \frac{4(t_L^* + r_L^*)^2 + 4(t_S^* + r_S^*)^2}{k+2}$.

Proof. Let us first make two simple observations.

Since $f(\mathbf{L}^*, \mathbf{S}^*) \leq g(\mathbf{L}^k, \mathbf{S}^k, t_L^k, t_S^k)$, we have

$$U_L^k = g(\mathbf{L}^k, \mathbf{S}^k, t_L^k, t_S^k) / \lambda_L \geq t_L^* \quad \text{and} \quad U_S^k = g(\mathbf{L}^k, \mathbf{S}^k, t_L^k, t_S^k) / \lambda_S \geq t_S^*. \quad (\text{D.5})$$

Therefore, our U_L^k and U_S^k always bound t_L^* and t_S^* from above.

From Lemma 5, $g(\mathbf{L}^k, \mathbf{S}^k, t_L^k, t_S^k)$ is non-increasing,

$$f(\mathbf{L}^k, \mathbf{S}^k) \leq g(\mathbf{L}^k, \mathbf{S}^k, t_L^k, t_S^k) \leq g(\mathbf{L}^0, \mathbf{S}^0, t_L^0, t_S^0),$$

which implies that $(\mathbf{L}^k, \mathbf{S}^k) \subseteq \overline{B(r_L^*)} \times \overline{B(r_S^*)}$, i.e. $\|\mathbf{L}^k\|_F \leq r_L^*$ and $\|\mathbf{S}^k\|_F \leq r_S^*$.

Let us now consider the k -th iteration. Similar to the proof in [HJN13], we introduce the auxiliary point $\mathbf{v}_+^k = (\frac{t_L^*}{U_L^k} \mathbf{V}_L^k, \frac{t_S^*}{U_S^k} \mathbf{V}_S^k, \frac{t_L^*}{U_L^k} \mathbf{V}_{t_L}^k, \frac{t_S^*}{U_S^k} \mathbf{V}_{t_S}^k)$. Then based on our argument for (4.13), it can be easily verified that

$$(\mathbf{L}[\mathbf{v}_+^k], t_L[\mathbf{v}_+^k]) \in \arg \min_{\|\mathbf{v}_L\|_* \leq V_{t_L} \leq t_L^*} g_L(\mathbf{V}_L, V_{t_L}) \quad (\text{D.6})$$

$$(\mathbf{S}[\mathbf{v}_+^k], t_S[\mathbf{v}_+^k]) \in \arg \min_{\|\mathbf{v}_S\|_1 \leq V_{t_S} \leq t_S^*} g_S(\mathbf{V}_S, V_{t_S}). \quad (\text{D.7})$$

Recall $\gamma = \frac{2}{k+2}$. We have

$$\begin{aligned}
& g(\mathbf{x}^{k+\frac{1}{2}}) \\
& \leq g(\mathbf{x}^k + \gamma(\mathbf{v}_+^k - \mathbf{x}^k)) \\
& \leq g(\mathbf{x}^k) + \gamma \langle \nabla g(\mathbf{x}^k), \mathbf{v}_+^k - \mathbf{x}^k \rangle + \gamma^2 \left(\|\mathbf{L}[\mathbf{v}_+^k] - \mathbf{L}[\mathbf{x}^k]\|_F^2 + \|\mathbf{S}[\mathbf{v}_+^k] - \mathbf{S}[\mathbf{x}^k]\|_F^2 \right) \\
& \leq g(\mathbf{x}^k) + \gamma \left(g_L(\mathbf{L}[\mathbf{v}_+^k] - \mathbf{x}^k], t_L[\mathbf{v}_+^k - \mathbf{x}^k]) + g_S(\mathbf{S}[\mathbf{v}_+^k] - \mathbf{x}^k], t_S[\mathbf{v}_+^k - \mathbf{x}^k]) \right) \\
& \quad + \gamma^2 \left((t_L^* + r_L^*)^2 + (t_S^* + r_S^*)^2 \right) \\
& \leq g(\mathbf{x}^k) + \gamma \left(g_L(\mathbf{L}[\mathbf{x}^* - \mathbf{x}^k], t_L[\mathbf{x}^* - \mathbf{x}^k]) + g_S(\mathbf{S}[\mathbf{x}^* - \mathbf{x}^k], t_S[\mathbf{x}^* - \mathbf{x}^k]) \right) \\
& \quad + \gamma^2 \left((t_L^* + r_L^*)^2 + (t_S^* + r_S^*)^2 \right) \\
& = g(\mathbf{x}^k) + \gamma \langle \nabla g(\mathbf{x}^k), \mathbf{x}^* - \mathbf{x}^k \rangle + \gamma^2 \left((t_L^* + r_L^*)^2 + (t_S^* + r_S^*)^2 \right) \\
& \leq g(\mathbf{x}^k) + \gamma \left(g(\mathbf{x}^*) - g(\mathbf{x}^k) \right) + \gamma^2 \left((t_L^* + r_L^*)^2 + (t_S^* + r_S^*)^2 \right),
\end{aligned}$$

where the first inequality holds since $\mathbf{x}^k + \gamma(\mathbf{v}_+^k - \mathbf{x}^k)$ is feasible to the quadratic program (4.18) while $\mathbf{x}^{k+\frac{1}{2}}$ minimizes it; the third inequality is due to the facts that

$$\begin{aligned}
\|\mathbf{L}[\mathbf{v}_+^k] - \mathbf{L}[\mathbf{x}^k]\|_F & \leq \|\mathbf{L}[\mathbf{v}_+^k]\|_F + \|\mathbf{L}[\mathbf{x}^k]\|_F \leq \|\mathbf{L}[\mathbf{v}_+^k]\|_* + \|\mathbf{L}[\mathbf{x}^k]\|_F \leq t_L^* + r_L^* \\
\|\mathbf{S}[\mathbf{v}_+^k] - \mathbf{S}[\mathbf{x}^k]\|_F & \leq \|\mathbf{S}[\mathbf{v}_+^k]\|_F + \|\mathbf{S}[\mathbf{x}^k]\|_F \leq \|\mathbf{S}[\mathbf{v}_+^k]\|_1 + \|\mathbf{S}[\mathbf{x}^k]\|_F \leq t_S^* + r_S^*;
\end{aligned}$$

the fourth inequality holds as $(\mathbf{L}[\mathbf{x}^*], t_L[\mathbf{x}^*])$ and $(\mathbf{S}[\mathbf{x}^*], t_S[\mathbf{x}^*])$ are respectively feasible to (D.6) and (D.7) while $(\mathbf{L}[\mathbf{v}_+^k], t_L[\mathbf{v}_+^k])$ and $(\mathbf{S}[\mathbf{v}_+^k], t_S[\mathbf{v}_+^k])$ respectively minimize (D.6) and (D.7);

Therefore, we obtain

$$g(\mathbf{x}^{k+\frac{1}{2}}) - g(\mathbf{x}^*) \leq (1 - \gamma) (g(\mathbf{x}^k) - g(\mathbf{x}^*)) + \gamma^2 \left((t_L^* + r_L^*)^2 + (t_S^* + r_S^*)^2 \right).$$

Moreover, by Lemma 5, we have

$$g(\mathbf{x}^{k+1}) \leq g(\mathbf{x}^{k+\frac{1}{2}}).$$

Thus, we obtain the recurrence

$$g(\mathbf{x}^{k+1}) - g(\mathbf{x}^*) \leq (1 - \gamma) (g(\mathbf{x}^k) - g(\mathbf{x}^*)) + \gamma^2 \left((t_L^* + r_L^*)^2 + (t_S^* + r_S^*)^2 \right),$$

Applying Lemma A.1 establishes that

$$g(\mathbf{L}^k, \mathbf{S}^k, t_L^k, t_S^k) - g(\mathbf{L}^*, \mathbf{S}^*, t_L^*, t_S^*) \leq \frac{4 \left((t_L^* + r_L^*)^2 + (t_S^* + r_S^*)^2 \right)}{k + 2}.$$

□

D.6 Proof of Theorem 6

Proof. Define $\Delta^k = g(\mathbf{x}^k) - g(\mathbf{x}^*)$. Following (D.2), we have

$$\Delta^{k+1} \leq \Delta^k + \gamma \langle \nabla g(\mathbf{x}^k), \mathbf{v}^k - \mathbf{x}^k \rangle + 4\gamma^2 \left((U_L^0)^2 + (U_S^0)^2 \right). \quad (\text{D.8})$$

Then following the arguments in the proof of Theorem 2 with (B.5) replaced by (D.8), we can easily obtain the result. □

E ISTA & FISTA for problem (1.5)

ISTA, a natural extension of the gradient method, can be used to solve problem (1.5),

$$\min \quad f(\mathbf{L}, \mathbf{S}) = l(\mathbf{L}, \mathbf{S}) + \lambda_L \|\mathbf{L}\|_* + \lambda_S \|\mathbf{S}\|_1,$$

where the data fidelity term $l(\mathbf{L}, \mathbf{S}) = \frac{1}{2} \|\mathcal{P}_\Omega[\mathbf{L} + \mathbf{S} - \mathbf{M}]\|_F^2$. In each iteration, ISTA updates (\mathbf{L}, \mathbf{S}) in the following manner,

$$(\mathbf{L}^{k+1}, \mathbf{S}^{k+1}) = \arg \min_{\mathbf{L}, \mathbf{S}} \left\langle \begin{pmatrix} \nabla_{\mathbf{L}} l(\mathbf{L}^k, \mathbf{S}^k) \\ \nabla_{\mathbf{S}} l(\mathbf{L}^k, \mathbf{S}^k) \end{pmatrix}, \begin{pmatrix} \mathbf{L} - \mathbf{L}^k \\ \mathbf{S} - \mathbf{S}^k \end{pmatrix} \right\rangle + \frac{L_f}{2} \left\| \begin{pmatrix} \mathbf{L} \\ \mathbf{S} \end{pmatrix} - \begin{pmatrix} \mathbf{L}^k \\ \mathbf{S}^k \end{pmatrix} \right\|_F^2 + \lambda_L \|\mathbf{L}\|_* + \lambda_S \|\mathbf{S}\|_1 \quad (\text{E.1})$$

Here $L_f = 2$ denotes the Lipschitz constant of $\nabla l(\mathbf{L}, \mathbf{S})$ with respect to (\mathbf{L}, \mathbf{S}) , and $\nabla_{\mathbf{L}} l(\mathbf{L}^k, \mathbf{S}^k) = \nabla_{\mathbf{S}} l(\mathbf{L}^k, \mathbf{S}^k) = \mathcal{P}_\Omega[\mathbf{L}^k + \mathbf{S}^k - \mathbf{M}]$. Since \mathbf{L} and \mathbf{S} are decoupled in (E.1), equivalently we have

$$\mathbf{L}^{k+1} = \arg \min_{\mathbf{L}} \left\| \mathbf{L} - \left(\mathbf{L}^k - \frac{1}{2} \mathcal{P}_\Omega[\mathbf{L}^k + \mathbf{S}^k - \mathbf{M}] \right) \right\|_F^2 + \lambda_L \|\mathbf{L}\|_*, \quad (\text{E.2})$$

$$\mathbf{S}^{k+1} = \arg \min_{\mathbf{S}} \left\| \mathbf{S} - \left(\mathbf{S}^k - \frac{1}{2} \mathcal{P}_\Omega[\mathbf{L}^k + \mathbf{S}^k - \mathbf{M}] \right) \right\|_F^2 + \lambda_S \|\mathbf{S}\|_1. \quad (\text{E.3})$$

The solution to problem (E.3) can be given explicitly in terms of the proximal mapping of $\|\cdot\|_1$ as introduced in Section 2.2, i.e.,

$$\mathbf{S}^{k+1} = \mathcal{T}_{\lambda_S/2} \left[\mathbf{S}^k - \frac{1}{2} \mathcal{P}_\Omega[\mathbf{L}^k + \mathbf{S}^k - \mathbf{M}] \right].$$

For a matrix \mathbf{X} and any $\tau \geq 0$, let $\mathcal{D}_\tau(\mathbf{X})$ denote the singular value threshold operator $\mathcal{D}_\tau(\mathbf{X}) = \mathbf{U} \mathcal{T}_\tau(\boldsymbol{\Sigma}) \mathbf{V}^*$, where $\mathbf{X} = \mathbf{U} \boldsymbol{\Sigma} \mathbf{V}^*$ is any singular value decomposition. It is not difficult to show [CCS10, MGC11] that the solution to problem (E.2) can be given explicitly by

$$\mathbf{L}^{k+1} = \mathcal{D}_{\lambda_L/2} \left[\mathbf{L}^k - \frac{1}{2} \mathcal{P}_\Omega[\mathbf{L}^k + \mathbf{S}^k - \mathbf{M}] \right].$$

Algorithm 7 summarizes our ISTA implementation for problem (2).

Algorithm 7 ISTA for problem (2)

- 1: **Initialization:** $\mathbf{L}^0 = \mathbf{0}, \mathbf{S}^0 = \mathbf{0}$;
 - 2: **for** $k = 0, 1, 2, \dots$ **do**
 - 3: $\mathbf{L}^{k+1} = \mathcal{D}_{\lambda_L/2} [\mathbf{L}^k - \frac{1}{2} \mathcal{P}_\Omega[\mathbf{L}^k + \mathbf{S}^k - \mathbf{M}]]$;
 - 4: $\mathbf{S}^{k+1} = \mathcal{T}_{\lambda_S/2} [\mathbf{S}^k - \frac{1}{2} \mathcal{P}_\Omega[\mathbf{L}^k + \mathbf{S}^k - \mathbf{M}]]$;
 - 5: **end for**
-

Regarding ISTA's speed of convergence, it can be proved that $f(\mathbf{L}^k, \mathbf{S}^k) - f^* = O(1/k)$, where f^* denotes the optimal value of problem (2).

FISTA, introduced in [BT09], is an accelerated version of ISTA, which leverages the idea of Nesterov’s optimal gradient scheme [Nes83]. For FISTA, a better convergence result, $f(\mathbf{L}^k, \mathbf{S}^k) - f^* = O(1/k^2)$, can be achieved with comparable computational cost. We summarize our FISTA implementation for problem (2) in Algorithm 8.

Algorithm 8 FISTA for problem (2)

```

1: Initialization:  $\hat{\mathbf{L}}^0 = \mathbf{L}^0 = \mathbf{0}$ ,  $\hat{\mathbf{S}}^0 = \mathbf{S}^0 = \mathbf{0}$ ,  $t_0 = 1$ ;
2: for  $k = 0, 1, 2, \dots$  do
3:    $\mathbf{L}^{k+1} = \mathcal{D}_{\lambda_L/2} \left[ \hat{\mathbf{L}}^k - \frac{1}{2} \mathcal{P}_\Omega[\hat{\mathbf{L}}^k + \hat{\mathbf{S}}^k - \mathbf{M}] \right]$ ;
4:    $\mathbf{S}^{k+1} = \mathcal{T}_{\lambda_S/2} \left[ \hat{\mathbf{S}}^k - \frac{1}{2} \mathcal{P}_\Omega[\hat{\mathbf{L}}^k + \hat{\mathbf{S}}^k - \mathbf{M}] \right]$ ;
5:    $t^{k+1} = \frac{1 + \sqrt{1 + 4(t^k)^2}}{2}$ 
6:    $\hat{\mathbf{L}}^{k+1} = \mathbf{L}^{k+1} + \frac{t^k - 1}{t^{k+1}} (\mathbf{L}^{k+1} - \mathbf{L}^k)$ ;
7:    $\hat{\mathbf{S}}^{k+1} = \mathbf{S}^{k+1} + \frac{t^k - 1}{t^{k+1}} (\mathbf{S}^{k+1} - \mathbf{S}^k)$ ;
8: end for

```

Partial SVD Note that in each iteration of either ISTA or FISTA, we only need those singular values that are larger than $\lambda_S/2$ and their corresponding singular vectors. Therefore, a partial SVD can be utilized to reduce the computational burden of a full SVD. Since most partial SVD software packages (e.g. PROPACK) require specifying in advance the number of top singular values and singular vectors to compute, we heuristically determine this number (denoted as sv^k) for each iteration. Specifically, let $d = \min\{m, n\}$, and svp^k denote the number of computed singular values that are larger than $\lambda_S/2$ in the k -th iteration. Similar to [TY11], in our implementation, we start with $sv^0 = d/10$, and adjust sv^k dynamically as follows

$$sv^{k+1} = \begin{cases} \min\{svp^k + 1, d\} & \text{if } svp^k < sv^k \\ \min\{svp^k + \text{round}(0.05 * d), d\} & \text{otherwise.} \end{cases}$$